הטכניון
מכון טכנולוגי לישראל
TECHNION
Israel Institute of Technology

ספריות הטכניון
The Technion Libraries

בית הספר ללימודי מוסמכים ע"ש ארווין וג'ואן ג'ייקובס
Irwin and Joan Jacobs Graduate School

©
All rights reserved to the author

This work, in whole or in part, may not be copied (in any media), printed, translated, stored in a retrieval system, transmitted via the internet or other electronic means, except for "fair use" of brief quotations for academic instruction, criticism, or research purposes only. Commercial use of this material is completely prohibited.

©
כל הזכויות שמורות למחבר/ת

אין להעתיק (במדיה כלשהי), להדפיס, לתרגם, לאחסן במאגר מידע, להפיץ באינטרנט, חיבור זה או כל חלק ממנו, למעט "שימוש הוגן" בקטעים קצרים מן החיבור למטרות לימוד, הוראה, ביקורת או מחקר. שימוש מסחרי בחומר הכלול בחיבור זה אסור בהחלט.

© Technion - Israel Institute of Technology, Elyachar Central Library

Distance-Constrained Formation Tracking Control

Oshri Rozenheck

© Technion - Israel Institute of Technology, Elyachar Central Library

© Technion - Israel Institute of Technology, Elyachar Central Library

Distance-Constrained Formation Tracking Control

Research Thesis

Submitted in partial fulfillment of the requirements
for the degree of Master of Science in the Technion
Autonomous Systems Program

Oshri Rozenheck

Submitted to the Senate
of the Technion — Israel Institute of Technology
Nisan 5776 Haifa April 2016

© Technion - Israel Institute of Technology, Elyachar Central Library

The research thesis was done under the supervision of Prof. Daniel Zelazo in the Technion Autonomous Systems Program.

The generous financial help Of Leonard and Diane Sherman is gratefully acknowledged.

List of publications based on this thesis:

- Oshri Rozenheck, Shiyu Zhao, and Daniel Zelazo. Distance-constrained formation tracking control. In *Israel 55th Annual Conference on Aerospace Sciences (IACAS)* , 2015.
- Oshri Rozenheck, Shiyu Zhao, and Daniel Zelazo. A proportional-integral controller for distance-based formation tracking. *European Control Conference (ECC), pages 1693-1698. IEEE* , 2015.

© Technion - Israel Institute of Technology, Elyachar Central Library

© Technion - Israel Institute of Technology, Elyachar Central Library

© Technion - Israel Institute of Technology, Elyachar Central Library

Acknowledgements

This thesis represents not only my work on the keyboard, but it is a milestone in more than six years of work at the Technion and specifically within the field of control. My experience at the Technion has been nothing short of amazing. Starting as an undergraduate student at the Aerospace faculty, and moving on to working in a defense systems company and simultaneously teaching undergraduate students as a TA, I learned that you need to push hard in order to succeed. Throughout these years I have learned that an educated man is one who never stops learning new things. This thesis is also the result of many great experiences I have encountered at the Technion and beyond, and from several remarkable individuals who I also wish to acknowledge.

First and foremost I would like to express my sincere appreciation to my supervisor, Prof. Dan Zelazo, director of the Cooperative Networks and Control (CoNeCt) laboratory, for giving me the opportunity to join his research team and for his guidance and help throughout all stages of my work. His passion for matrices was the source of my inspiration to research large scale systems. I deeply acknowledged his caring beyond my academic needs and letting me work my way through the research on my own pace. His sincere insights on life were valuable to me as much as the pearls of wisdom he shared with me regarding the research. I would also like to thank him for teaching me that a hobby can be a major part of life and that sometimes the best lessons are given not as a supervisor, but as a my friend. when you read this, know that your smile truly makes a difference.

I am also immensely grateful to my colleague Dr. Shiyu Zhao for supporting my research and for giving me numerous ideas and leading directions when difficult times came.

I gratefully acknowledge the generous financial support of the Technion and the Israel Science Foundation.

I finish with home, where the most basic source of my life energy resides: my wife, Shimrit. Her support has been unconditional all these years. She have cherished with me every great moment and supported me whenever I needed it. I would like to express gratitude for her love, patience, support, help, advice and encouragement during my studies. I could have not done it without her.

© Technion - Israel Institute of Technology, Elyachar Central Library

© Technion - Israel Institute of Technology, Elyachar Central Library

Contents

© Technion - Israel Institute of Technology, Elyachar Central Library

© Technion - Israel Institute of Technology, Elyachar Central Library

List of Figures

© Technion - Israel Institute of Technology, Elyachar Central Library

© Technion - Israel Institute of Technology, Elyachar Central Library

Nomenclature

δ_e	Formation distance error vector	$E(\mathcal{G})$	Incidence Matrix of graph $\mathcal{G}$
δ_{ref}	Velocity reference error vector	$F(x, \mathcal{G})$	Edge Function
δ_v	Velocity error vector	I	Identity matrix
κ_I	Proportional Integrator gain	$L(\mathcal{G})$	Laplacian of graph $\mathcal{G}$
κ_P	Proportional gain	m	Size of a graph
$\mathbb{R}$	Set of real numbers	MIR	Minimally infinitesimally rigid
$\mathcal{E}$	Edge set	n	Order of a graph
$\mathcal{G}$	Graph	$R(x)$	Rigidity matrix
$\mathcal{N}_i$	Neighborhood of i	u_i	Control input of agent i
$\mathcal{R}(x)$	Symmetric rigidity matrix	$V(x)$	Lyapunov function
$\mathcal{V}$	Vertex set	v_i	Velocity vector of agent i
$\mathbf{1}$	All ones vector	v_{ref}	Reference velocity vector
d	Distance constraints vector	x_i	Position vector of agent i

© Technion - Israel Institute of Technology, Elyachar Central Library

© Technion - Israel Institute of Technology, Elyachar Central Library

Abstract

This work considers a multi-agent formation control problem where a designated leader is subjected to an additional velocity reference command. The entire formation should follow the leader while maintaining the inter-agent distance constraints. The formation error is defined from the zero-input dynamics of agents modeled as single integrators. A local stability proof is provided by using the dynamics of the formation error and employing Lyapunov's indirect method. Finding an upper bound on the steady state error of the linearized dynamics also reveals significant relations between the error properties to those of the graph topology. By augmenting a standard gradient formation controller with a proportional-integral control on the formation error, we are able to prove the stability of the formation error dynamics with velocity input while ensuring zero steady-state formation error. To agents with double integrator dynamics we add a consensus-based control loop on the velocities to achieve the formation maintenance problem. The formation error is augmented with a velocity error, that defines the differences between the velocity of each agent to that of the reference. Lyapunov's second method is used to prove that the system is asymptotically stable. For a system with an external reference velocity a decentralized control is proposed to manipulate the agents' velocities and a velocity feedback mechanism is implemented on the leader to assure the formation tracks the reference signal. Numerical simulations are shown to illustrate the theoretical results.

© Technion - Israel Institute of Technology, Elyachar Central Library

© Technion - Israel Institute of Technology, Elyachar Central Library

Chapter 1

Introduction

Multi-agent systems (MAS) are systems composed of multiple interacting intelligent agents within some environment. MAS can be used to solve different problems that are difficult or even impossible for an individual to solve, and are applied in many areas in the real world, such as computer games [7, 28], animations [24, 33], coordinated defence systems [30, 32, 47], transportation [10, 27] and so on. Many different areas of research for multi-agents systems have emerged in the last years and this thesis is aiming to investigate how to control and manipulate such systems.

In particular, the thesis will discuss on how to control a formation of a group of agents when one of them is subjected to an external input, which aimed at driving the formation with a desired velocity. The motivation for the thesis comes from a real-world task that deals with a formation of several autonomous surface vehicles (ASV) that can communicate with each other in different ways such as radio, microwaves or free-space optical communication. Their main goal is to reach a specified destination in a harsh environment, such as a rocky mountain, tall grass or an urban environment, while staying in a formation shape. Due to various area features the vehicles cannot communicate with the operator all the time. For that purpose one of the agents communicates with a remote controlled unmanned aerial vehicle (UAV) that hovers above it and transmits back instructions, such as the next destination or velocity changes.

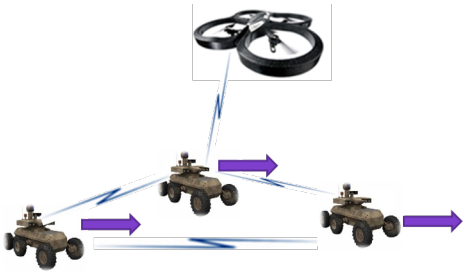

Figure 1.1: Formation tracking mission. The drone communicates with the leader only, while the other USVs required to stay in a fromation shape. .

The real problem arises when the UAV is moving in a constant velocity towards a new location. The leader, and subsequently the rest of the ground agents, have to follow it quickly while preserving the formation shape (see Figure 1.1). Without the presence of any additional control, such change in the velocity can be interpreted as a disturbance to the agents' dynamics, causing the followers to fall behind the leader. The lag implication can be reflected as an undesired change of the inter-agents distances and it will be discussed thoroughly in the thesis.

1.1 Literature Review

In recent years, there has been much attention given to the control of formations of multiple agents across many application domains. Of the many control strategies for formation control, distance-constrained formation stabilization has been extensively studied [2, 3, 8, 14, 17, 22, 31, 50]. A closely related problem is formation tracking where the objective is to find a control scheme that allow multiple robots to maintain some given formation while executing additional tasks such as velocity tracking or leader following.

Distance-constrained formation control aims at maintaining inter-agent distances and utilizes relative measurements (i.e., distances and relative-positions) to generate the control action. The theory of rigidity has emerged as the correct mathematical foundation for defining distance-constrained formations and proving that distance-constrained formation control strategies are stabilizing [1, 3, 5]. Rigidity theory is also concerned with properties of graphs that ensure that the formation modeled by the graph is rigid. Roughly speaking, a formation is rigid if the only distance-preserving motions of the ensemble are the rigid-body rotations and translations of the entire formation. For the precise definition of rigidity and broader overview of graph rigidity, see [3, 5, 6].

In addition to conventional approaches where the target formation is defined by relative positions or distances, [16, 52, 53] propose bearing-based approach where the target formation is defined by inter-neighbor bearings. Additionally, a comprehensive review formation control that is based on the graph Laplacian is provided in [36]. The PI controllers are known for their successful attenuation of constant disturbances in the network, and hence can serve as a working point in formation maintenance and tracking problems. The authors in [4, 23] propose a distributed proportional-integral controller for the consensus of networked dynamical systems, while [53] present a proportional integral controller approach for bearing-based formation control in the presence of input disturbances. In this work, the use of a PI controller is introduced in order attain velocity tracking of the formation.

The stability analysis of these control strategies has been investigated in many works. In [21], application of the center manifold theorem was used to prove the local stability of infinitesimally rigid formations. Lyapunov-based approaches were employed in [14, 15] and a

© Technion - Israel Institute of Technology, Elyachar Central Library

general formation control scheme by using the error dynamics was presented in [37].

Despite its apparent utility, there are very few existing studies addressing velocity tracking in formation control. The aid of one or more virtual agents to help the formation achieve a desired common velocity or to arrive at a desired destination is considered in [42, 43, 45]. In particular, [30] proposed a flocking algorithm with a virtual leader by including a navigational feedback mechanism to every agent under the assumption that all agents are being informed.

Multi-agent systems with double integrator dynamics are also discussed in the literature. Necessary and sufficient conditions for second-order consensus are described in [48, 49], and general consensus protocol is investigated in [34]. Stability analysis of second order systems is discussed in [14, 44, 45].

The formation tracking problem for agents with double integrator dynamics are not so common in literature, but some work has been done. In [36] maneuvering of the flocking agents was achieved by adding a dynamic virtual leader dependent term to the control scheme. In [12] the presented distributed control architecture employs static output feedback using an artificial delay, whereas [11] present a distributed containment control.

1.2 Thesis Contributions

In this work, we first consider a collection of agents with integrator dynamics tasked with maintaining a distance-constrained formation. As a first contribution of our work, we provide an alternative local stability proof by deriving the dynamics of the formation error and employing Lyapunov's indirect method. Relations between the error properties to those of the graph are revealed in order to find an upper bound for the linearized steady-state error.

One agent in the ensemble is also designated as a leader and is subjected to an external velocity reference command. In the absence of any additional control action, the standard rigidity based formation stabilization solutions will exhibit a steady-state formation error. To address this, we augment the gradient based formation controller with a proportional and integral (PI) control on the formation error. We show that such a scheme preserves the stability properties of the formation error dynamics while ensuring a zero steady-state formation error. This scheme has many advantages, including a simple and distributed implementation and no need for virtual leaders.

As a second phase, we examine the formation error for agents with double integrator dynamics, tasked with the same formation maintenance problem. We notice that a stabilizing controller (an acceleration level input) is also needed for eliminating the steady state formation error. We show that by closing a consensus based control loop on the velocities of the agents we are able to achieve velocity consensus.

To analyze the system's stability, the same technique is employed to derive an appropriate

© Technion - Israel Institute of Technology, Elyachar Central Library

error of the dynamical system. The stability properties of the error dynamics are studied and a local stability proof is provided by using Lyapunov's direct method.

The main goal of the external velocity input is to determine the velocity of the formation as a whole, meaning that each agent should have a steady state velocity equal to that of the reference. For the second order system, such input will cause the agents to move in a formation shape but with a different velocity than that of the reference. For that purpose the difference between the velocity of the leader to the reference velocity is added to the leader's control law as a control gain to attain the reference velocity. The remaining agents are not aware of the external reference velocity but with the proposed control mechanism they are able to achieve the required external velocity.

1.3 Thesis Organization

The organization of this work is as follows. Chapter 2 reviews some fundamental concepts and notations from graph theory, rigidity theory and stability theory. In Chapter 3, the main problem statement is formally described.

The well known distance-constrained formation control law is applied on agents with single integrator dynamics and is presented in Chapter 4. Then, the formation distance error dynamics is derived in Section 4.1 and the stability analysis of the system is discussed. A control mechanism for the dynamics with velocity reference is presented in Section 4.2. This section also includes stability and performance analysis of the proportional controller and the PI controller.

Double integrator dynamics are introduced in Chapter 5, and the suitable error dynamics is presented in Section 5.1. The error is now augmented from the formation distance error and the new defined velocity error in order to stabilize the system. A more extensive analysis of the second order formation stability is shown in Section 5.1.1. In order to deal with an external reference velocity into the system, an inner control loop is implemented on the leader as can be read in Section 5.2. Stability proof for the closed loop dynamics is also provided in that section.

Numerical simulations are given along the thesis to verify the theoretical results. Finally, Chapter 6 contains concluding remarks and areas for future work.

© Technion - Israel Institute of Technology, Elyachar Central Library

© Technion - Israel Institute of Technology, Elyachar Central Library

Chapter 2

Preliminaries

This chapter reviews basic notations and provides sufficient graph theory background. Dealing with control algorithms in this thesis, such as formation control and tracking, relies on some basic concepts of rigid graph theory and on some key results from stability theory, which are also outlined below. An indepth coverage of these concepts can be found in [19, 20, 25, 29].

2.1 Notations

Given $A_1, \ldots, A_n \in \mathbb{R}^{p\times q}$, when the range of i is clear from the context, denote $\mathrm{diag}(A_i) \triangleq \mathrm{blkdiag}\{A_1, \ldots, A_n\} \in \mathbb{R}^{np\times nq}$. Denote I_n as the $n\times n$ identity matrix. Let $\mathbf{1}_n = [1, \ldots, 1]^{\mathrm{T}} \in \mathbb{R}^n$ be the vectors of all ones. The eigenvalues of a symmetric positive semi-definite matrix A are denoted as $0 \leq \lambda_1(A) \leq \lambda_2(A) \leq \cdots \leq \lambda_n(A)$. The matrix Kronecker product is useful when more than 1 dimension are involved. The Kronecker product of matrices $A \in \mathbb{R}^{n\times m}$ and $B \in \mathbb{R}^{p\times q}$ is given as

$$A \otimes B = \begin{bmatrix} a_{11}B & \cdots & a_{1m}B \\ \vdots & \ddots & \vdots \\ a_{n1}B & \cdots & a_{nm}B \end{bmatrix},$$

where a_{ij} denotes the ij-th entry of the matrix A. The following Kronecker product matrix multiplication will also be extensively used:

$$(A \otimes B)(C \otimes D) = AC \otimes BD,$$

where the matrices are all of commensurate dimensions. The range of $A \in \mathbb{R}^{m\times n}$, denoted as $Range(A)$, is the span (set of all possible linear combinations) of its column vectors. The rank of a matrix A, denoted as $rank(A)$, is the dimension of the vector space spanned by its columns or rows. A matrix is said to have $full\ rank$ if its rank equals the largest possible for a matrix of the same dimensions, which is the lesser of the number of rows and columns. The null space

© Technion - Israel Institute of Technology, Elyachar Central Library

of matrix A, denoted as $Null(A)$, is the set of vectors which are sent to the zero vector by A. That is, $Null(A) = \{v \in \mathbb{R}^n \mid Av = 0\}$.

2.2 Graph Theory

Graph theory is the study of graphs, which are mathematical structures used to model pairwise relations between objects [19, 25]. A graph $\mathcal{G} = (\mathcal{V}, \mathcal{E})$ in this context consists of a vertex set $\mathcal{V}$ and an edge set $\mathcal{E} \subseteq \mathcal{V} \times \mathcal{V}$. We denote the number of nodes in a graph as $n \triangleq |\mathcal{V}|$ (the *order* of a graph) and the number of edges as $m \triangleq |\mathcal{E}|$ (the *size* of a graph). If $(i, j) \in \mathcal{E}$ is an edge of a graph $\mathcal{G} = (\mathcal{V}, \mathcal{E})$, then i and j are said to be *adjacent*. The set of neighbors of vertex i is denoted as $\mathcal{N}_i \triangleq \{j \in \mathcal{V} : \ (i, j) \in \mathcal{E}\}$, and also noted as $i \sim j$. A *spanning tree* is a connected graph with $|\mathcal{V}| - 1$ edges. A graph is called *undirected*, when there is no distinction between the two vertices associated with each edge, i.e., an edge (i, j) is an unordered pair of distinct nodes i and j. An *orientation* of an undirected graph is the assignment of a direction to each edge and an *oriented graph* is an undirected graph whose edges are assigned with an ordered pair of vertices. For an edge (i, j), we say that an edge is from its *tail*, vertex i, to its *head*, vertex j. These vertices together are called *endpoints* of the edge. By assigning an arbitrary orientation to an undirected graph we can define the incidence matrix. The *incidence matrix* $E(\mathcal{G}) \in \mathbb{R}^{n \times m}$ of an oriented graph (sometimes reffered to as E) is the $\{0, \pm 1\}$ matrix with rows indexed by vertices and columns by edges. Let $\mathcal{G}$ be a directed graph with edge set $\mathcal{E} = \{e_1, ..., e_m\}$ and vertex set $\mathcal{V} = \{v_1, ..., v_n\}$. For directed graphs without self-loops, the elements of the incidence matrix of $\mathcal{G}$ are defined by

$$[E(\mathcal{G})]_{ij} = \begin{cases} -1 & if\ v_i\ is\ the\ tail\ of\ e_j, \\ 1 & if\ v_i\ is\ the\ head\ of\ e_j, \\ 0 & otherwise. \end{cases}$$

For any connected graph, it then follows that $\mathrm{Null}\,(E(\mathcal{G})^{\mathrm{T}}) = \mathrm{span}\{\mathbf{1}_n\}$ [19]. The *Laplacian* of a graph is a matrix defined as $L(\mathcal{G}) = E(\mathcal{G})E(\mathcal{G})^T$. Note that the product $E(\mathcal{G})E(\mathcal{G})^T$ is independent of the chosen orientation of the edges of $\mathcal{G}$. In this work we assume that the communication method between two identical agents is reciprocal. For that reason, and due to the fact that $L(\mathcal{G})$ is orientation-independent, we mainly deal with undirected graphs. Also, by definition, $L(\mathcal{G})$ is a real symmetric matrix and also positive semi-definite. Therefore it has n non-negative real eigenvalues ordered as $0 = \lambda_1(L(\mathcal{G})) \leq \lambda_2(L(\mathcal{G})) \leq ... \leq \lambda_n(L(\mathcal{G}))$ (repeated according to their multiplicities). It is easy to see that 0 is always an eigenvalue of $L(\mathcal{G})$ and that $\mathbf{1}_n$ is the corresponding eigenvector. Furthermore, the multiplicity of the zero eigenvalue of the graph Laplacian is equal to the number of connected components of the graph [19].

© Technion - Israel Institute of Technology, Elyachar Central Library

Moreover, the second smallest eigenvalue of $L(\mathcal{G})$, $\lambda_2(L(\mathcal{G}))$ is also known as the algebraic connectivity of the graph [18].

2.3 Rigidity Theory

Rigidity theory plays an important role in distance-based formation control. We next review some important definitions and results from rigidity theory; for a more detailed review, see [3, 5].

A d-dimensional *configuration* is a finite collection of n points, $x = [x_1^{\mathrm{T}}, \ldots, x_n^{\mathrm{T}}]^{\mathrm{T}} \in \mathbb{R}^{dn}$, where $x_i \in \mathbb{R}^d$ and $x_i \neq x_j$ for all $i \neq j$. A *framework*, denoted as $\mathcal{G}(x)$, is an undirected graph $\mathcal{G}$ together with a configuration x, where vertex i in the graph is mapped to the point x_i. Oriented graphs turn out to be useful when discussing and studying frameworks rigidity. Let $(i, j) \in \mathcal{E}$ correspond to the k-th directed edge in the orientation of graph $\mathcal{G}$. Define the edge vector for a framework, sometimes called the relative position vector, as $e_k \triangleq x_j - x_i$. The edges vector of the entire framework can be denoted as $e = \begin{bmatrix} e_1^{\mathrm{T}} \cdots e_m^{\mathrm{T}} \end{bmatrix}^{\mathrm{T}} \in \mathbb{R}^{2m}$.

Two frameworks $\mathcal{G}(x)$ and $\mathcal{G}(y)$ in $\mathbb{R}^2$ are *equivalent* if $\|x_i - x_j\| = \|y_i - y_j\|$ for all $\{(i, j)\} \in \mathcal{E}$. Two frameworks $\mathcal{G}(x)$ and $\mathcal{G}(y)$ in $\mathbb{R}^2$ are *congruent* if $\|x_i - x_j\| = \|y_i - y_j\|$ for all $i, j \in \mathcal{V}$. Two frameworks can be equivalent but not congruent. An example with two frameworks is described in Figure 2.1, where the distances of every edge in the edge set are similar in both frameworks, but the distance between node 2 and node 4 is different in each framework. Thus, the two frameworks are equivalent but not congruent.

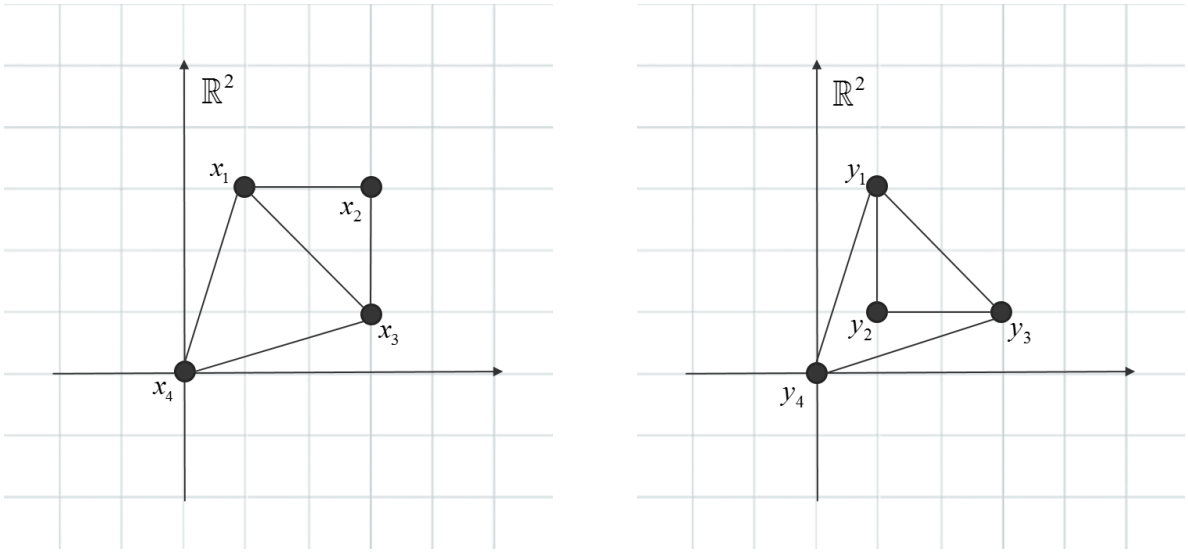

(a) Framework 1. (b) Framework 2.

Figure 2.1: Two frameworks which are equivalent but not congruent.

A framework $\mathcal{G}(x)$ is *rigid* if there exists an $\epsilon > 0$ such that if framework $\mathcal{G}(y)$ is equivalent to $\mathcal{G}(x)$ and satisfies $\|y_i - x_i\| \leq \epsilon$ for all $i \in \mathcal{V}$, then $\mathcal{G}(y)$ is congruent to $\mathcal{G}(x)$. A framework $\mathcal{G}(x)$ is *globally rigid* if every framework that is equivalent to $\mathcal{G}(x)$ is also congruent to $\mathcal{G}(x)$. Clearly, global rigidity implies rigidity. Figure 2.1 for example, illustrates a framework that is rigid but not globally rigid. Nevertheless, rigid frameworks can be converted to globally rigid frameworks by including additional distance constraints [3].

Graph rigidity can also be interpreted upon the notion of bar-and-joint frameworks where the distances between nodes are assumed to be fixed. We are interested in whether there is a motion or deformation of this structure that preserves the lengths of the bars and the points of attachment between the bars and joints but gives a genuine change in the shape of the structure, i.e., a change in the distance between two joints that does not define an edge. When no such motion exists the structure is rigid.

Given an arbitrary oriented graph, consider a framework $\mathcal{G}(x)$ with the edge vectors as $\{e_k\}_{k=1}^m$. Define the *edge function*, $F : \mathbb{R}^{2n} \times \mathcal{G} \to \mathbb{R}^m$, as a transformation from the configuration of the graph to its edge-square-length, as

$$F(x, \mathcal{G}) \triangleq \left[\|e_1\|^2, \ldots, \|e_m\|^2\right]^T.$$

Note that the edge function is not unique and it depends on the ordering given to the edges. If $F(p, \mathcal{G}) = F(q, \mathcal{G})$ for $p, q \in \mathbb{R}^2$, then the corresponding edges of framework $\mathcal{G}(p)$ and $\mathcal{G}(q)$ have the same length, i.e., the frameworks are equivalent.

The *rigidity matrix* $R(x)$, associated with a framework $\mathcal{G}(x)$, is the Jacobian of the edge function, $R(x) \triangleq \partial F(x, \mathcal{G})/\partial x \in \mathbb{R}^{m \times 2n}$. The rigidity matrix encapsulates some of the rigidity properties of a framework and it is discussed shortly. A short calculation shows that $R(x)$ can be equivalently written as

$$R(x) = \mathrm{diag}(e_i^{\mathrm{T}})(E^{\mathrm{T}} \otimes I_2). \tag{2.1}$$

This representation separates the graph from the positions of the nodes. The *symmetric rigidity matrix* associated with a framework $\mathcal{G}(x)$ is the $2n \times 2n$ matrix defined as $\mathcal{R}(x) \triangleq R(x)^{\mathrm{T}} R(x)$ [50].

If $dx \in \mathbb{R}^{2n \times 1}$ satisfies $R(x)dx = 0$, then dx is called an *infinitesimal flex* of $\mathcal{G}(x)$. In Figure 2.2(a) we have a non-rigid framework, where a non-trivial motion causes a change in the distance between a pair of nodes, although the bars constraints are preserved. A Framework $\mathcal{G}(x)$ is *infinitesimally rigid* if the only infinitesimal flexes are trivial, i.e., the rigid body rotations and translations of the framework. Such frameworks are described in Figures 2.2(b) and 2.2(c), where every flex motion is distance preserving. As the definition suggest, infinitesimal rigidity does imply rigidity. rigidity of graphs is a generic property in the sense that almost

© Technion - Israel Institute of Technology, Elyachar Central Library

all realizations of a particular graph are either infinitesimally rigid, or flexible. A *minimally rigid graph* is a rigid graph such that the removal of any edge results in a non-rigid graph. As an example, the graph in Figure 2.2(b) is a minimally rigid graph whereas the graph in Figure 2.2(c) is not. This property can be mathematically interpreted if the rigid graph has $2n-3$ edges. A framework $\mathcal{G}(x)$ is *minimally infinitesimally rigid* (MIR) if it is infinitesimally rigid and the number of edges is $m = 2n-3$. As demonstrated in Figure 2.2(b), a graph consists of 4 agents and 5 edges will result in an MIR framework. In fact, the rigidity of a framework can

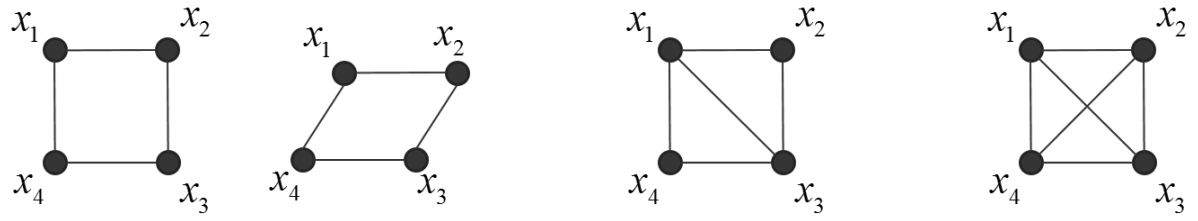

(a) A non-rigid framework. (b) MIR framework. (c) Infinitesimally rigid framework.

Figure 2.2: Rigidity of frameworks.

be characterized in terms of the rank of the rigidity matrix.

Lemma 1. *([46]) A framework $\mathcal{G}(x)$ is infinitesimally rigid if and only if $rank(R(x)) = 2n-3$.*

Since there are $2n-3$ edges in an MIR framework, the number of rows of the rigidity matrix must also be $2n-3$, leading to the following corollary.

Corollary 1. *If a framework is MIR, then the rigidity matrix $R(x)$ has full row rank.*

Corollary 1 gives a sufficient condition for the rigidity matrix of a framework having full row rank. The notion of MIR frameworks and Corollary 1 turn out to be an important property for deriving the stability of distance-constrained formation problems [13]. For that reason, those results will be exploited when stability of dynamic systems is discussed.

2.4 Stability Theory

Stability was probably the first question in classical dynamical systems that motivated the introduction of new mathematical concepts in engineeering and particularly in control engineering. Stability means that the trajectories of the output do not change too much under small perturbations from a given initial conditions or equilibrium state. Our treatment of stability will apply to control systems described by sets of linear or nonlinear equations. Consider the nonlinear autonomous (no forcing input) system

$$\dot{x}(t) = f(t, x(t)), \tag{2.2}$$

© Technion - Israel Institute of Technology, Elyachar Central Library

where $x : \mathbb{R} \to \mathbb{R}^n$ and $f : \mathbb{R} \times \mathbb{R}^n \to \mathbb{R}^n$ are functions and t, which usually represents time, is the only independent variable. The derivative $\dot{x}(t)$ is simply the derivatives of each of the component functions, so if $x(t) = (x_1(t), ..., x_n(t))$ where $x_i(t)$ are real-valued functions on $\mathbb{R}$ then,

$$\dot{x}(t) = (\dot{x}_1(t), ..., \dot{x}_n(t)).$$

It is essential to first discuss the stability of the autonomous case where there is no external driving force,

$$\dot{x}(t) = f(x(t)), \tag{2.3}$$

where $f : \mathbb{R}^n \to \mathbb{R}^n$. We are going to assume the existence of continuous solutions and uniqueness of a solution with the initial condition $x(t_0) = x_0$ where t_0 is a constant and x_0 is a constant n-vector.

The equilibrium points of (2.3) are constant solutions to the differential equations set and can be evaluated by setting all system derivatives to zero. We would like to characterize if the equilibrium point $\bar{x}(t)$ is stable. Stability is a qualitative notion that if we perturb a system from its equilibrium conditions slightly, say $\bar{x}(t_0) = \bar{x}_0 + \varepsilon$, then the trajectories generated by the dynamics in (2.3) will not change much [39]. We assume that $\bar{x}(t)$ is the origin of state space and we can formalize stability with the following mathematical theorem (without any loss of generality, since we can always do a state transformation with a new variable and study the stability of the new system with respect to it). There is no single concept of stability, and many different definitions are possible. We shall consider only several fundamental statements.

Theorem 1. Lyapunov Stability [20]: *The equilibrium $x(t) = 0$ of (2.3) is:*

1. Lyapunov stable, if for each $\epsilon > 0$ there exists a $\delta > 0$ such that

$$\|x(t_0)\| < \delta \Rightarrow \|x(t)\| < \epsilon, \quad \forall t > t_0.$$

2. Asymptotically stable if it is stable and in addition δ can be chosen such that

$$\|x(t_0)\| < \delta \Rightarrow \lim_{t \to \infty} \|x(t)\| = 0.$$

In general, asymptotic stability is more desirable, since the trajectories starting from initial conditions close to the origin will approach the origin asymptotically. Analyzing the stability of solutions to ordinary differential equations can be done by two main methods. First, the indirect method of Lyapunov uses the linearization of a system to determine the local stability of the original system. The second method, the Lyapunov direct method, uses an auxilliary function to find stability without having to characterize the solutions.

© Technion - Israel Institute of Technology, Elyachar Central Library

© Technion - Israel Institute of Technology, Elyachar Central Library

2.4.1 Lyapunov's First Method

Lyapunov's First Method, also known as the indirect method, works by characterizing solutions to differential equations of the type (2.3) and considering the properties of the linearized system. Those characterizations are used to infer about the system's stability. Let $x(t) = 0$ be an equilibrium point (2.3) where $f : D \to \mathbb{R}^n$ is a continuously differentiable and D is a neighborhood of the origin.

Theorem 2. *[20] Let $A = \frac{\partial f}{\partial x}\big|_{x=0}$, then*

1. The origin of (2.3) is asymptotically stable if $Re(\lambda_i) < 0$ for all eigenvalues of A. In that case, the matrix A is also called Hurwitz or asymptotically stable.

2. The origin of (2.3) is unstable if $Re(\lambda_i) > 0$ for one or more of the eigenvalues of A.

Theorem 2 does not say anything when $Re(\lambda_i) \leq 0, \forall i$ with $Re(\lambda_i) = 0$ for some i. In this case linearization fails to determine the stability of the equilibrium point, and further analysis is necessary. The multi-dimensional result which is relevant here is the Center Manifold Theorem but the reader is refer to [40] for further reading.

2.4.2 Lyapunov's Second Method

Lyapunov's Second or Direct Method does not require a characterization of the solutions to determine stability. The method is a generalization of the idea that if there is some measure of energy in a system, then we can study the rate of change of the energy of the system to ascertain stability.

The method uses a function, called the Lyapunov function, to determine properties of the asymptotic behavior of solutions to a differential equation of the general form (2.3). Let $V : D \to \mathbb{R}$ be a continuously differentiable function defined on the domain $D \subset \mathbb{R}^n$ that contains the origin. The rate of change of V along the trajectories of (2.3) is given by

$$\dot{V}(x(t)) = \frac{d}{dt}V(x(t)) = \sum_{i=1}^{n} \frac{\partial V}{\partial x_i}\frac{d}{dt}x_i = \begin{bmatrix} \frac{\partial V}{\partial x_1} & \frac{\partial V}{\partial x_2} & \cdots & \frac{\partial V}{\partial x_n} \end{bmatrix} \dot{x} = \frac{\partial V}{\partial x} f(x(t)). \quad (2.4)$$

The main idea of Lyapunov's theory is to establish properties of the nonlinear system by studying how certain carefully selected scalar functions of the state evolve as the system state evolves. In particular, the rate of change of the function $V(x)$ along any trajectory is as $x(t)$ varies according to (2.3). If $\dot{V}(x(t))$ is negative along the trajectories of the system, then $V(x(t))$ will decrease as time goes forward. Moreover, we do not really need to solve the nonlinear ODE (2.3) for every initial condition, but we just need some information about the drift $f(x(t))$. If such a function V exists, then stable solutions to the differential equation can be found. We are now ready to state Lyapunov's stability theorem.

© Technion - Israel Institute of Technology, Elyachar Central Library

Theorem 3. *[20] Let the origin $x(t) = 0 \in D \subset \mathbb{R}^n$ be an equilibrium point of (2.3). Let $V : D \to \mathbb{R}$ be a continuously differentiable function such that*

1. $V(0) = 0$
2. $V(x(t)) > 0, \forall x(t) \in D \backslash \{0\}$
3. $\dot{V}(x(t)) \leq 0, \forall x(t) \in D$.

Then, $x(t) = 0$ is a stable solution of (2.3). Moreover, if $\dot{V}(x(t)) < 0, \forall x(t) \in D \backslash \{0\}$, then $x(t) = 0$ is asymptotically stable.

If $V(x(t)) > 0, \forall x(t) \in D \backslash \{0\}$, then V is called locally positive definite. If $V(x(t)) \geq 0, \forall x(t) \in D \backslash \{0\}$, then V is locally positive semi-definite. If the conditions in Theorem 3 are met, then V is called a Lyapunov function for the system described in (2.3). Unfortunately, Lyapunov's theorem assumes the existence of a Lyapunov function, but does not provide any method to construct one from the differential equation (2.3). For proof, extensions and further examples, please refer to [20].

2.4.3 LaSalle's Invariance Principle

Lyapunov's method is extremely valuable, since it enables us to reach conclusions about stability without obtaining explicit solutions. The disadvantage is that finding an appropriate Lyapunov function can often be very difficult. Furthermore, when $\dot{V}(x)$ is a negative definite function, asymptotic stability of the origin is a direct consequence of Lyapunov's second theorem, but a criterion for asymptotic stability in the case when $\dot{V}(x)$ is only negative semi-definite is still missing.

In response to this fact, LaSalle produced an extension of Lyapunov's method. In this extension, LaSalle used the notion of limit sets and the notion of invariance (the property of certain sets whereby a given function takes elements in the set to elements in the same set). By introducing these notions, LaSalle was able to show how Lyapunov functions could be defined less restrictively.

LaSalle's theorem enables one to conclude asymptotic stability of an equilibrium point even when $\dot{V}(x)$ is negative semi-definite. We begin by introducing a few more definitions. We denote the solution trajectories of the autonomous system in (2.3) as $s(t, x_0, t_0)$, which is the solution at time t starting from x_0 at t_0. The $\omega - limit\ set$ is the set $S \subset \mathbb{R}^n$ of a trajectory $s(\cdot, x_0, t_0)$ if for every $y \in S$, there exists a strictly increasing sequence of times t_n such that

$$s(t_n, x_0, t_0) \to y$$

as $y \to \infty$. A (positively) $invariant\ set$ is the set $M \subset \mathbb{R}^n$ if for all $y \in M$ and $t_0 \geq 0$, we have

$$s(t_n, x_0, t_0) \in M \quad \forall t \geq t_0.$$

It may also be proved that the $\omega - limit\ set$ of every trajectory is closed and invariant. We may now state LaSalle's principle.

Theorem 4. *Let $V : \mathbb{R}^n \to \mathbb{R}$ be a locally positive definite function such that on the compact set $\Omega_c = \{x \in \mathbb{R}^n : V(x) \leq c\}$ we have $\dot{V}(x) \leq 0$. Define*

$$S = \left\{ x \in \Omega_c : \dot{V}(x) = 0 \right\}.$$

As $t \to \infty$, the trajectory tends to the largest invariant set inside S, i.e., its $\omega - limit\ set$ is contained inside the largest $invariant\ set$ in S. In particular, if S contains no invariant sets other than $x = 0$, then 0 is asymptotically stable.

For proof please refer to [20, 26].

© Technion - Israel Institute of Technology, Elyachar Central Library

© Technion - Israel Institute of Technology, Elyachar Central Library

© Technion - Israel Institute of Technology, Elyachar Central Library

Chapter 3

Formation Tracking - Problem Formulation

This chapter formalize the current methods for controlling a group of agents tasked with formation acquisition. When the leader is subjected to an external velocity input, the formation will exhibit a steady-state distance error. Hence, our main objective is to track an external reference velocity of the leader while maintaining the inter-agent distances. The need for further control modifications of the existing approach is emphasized here in order to solve the non-zero steady-state error problem, both for first and second order systems. In this work two different agent models are considered, single integrator and double integrator. Moreover, current gradient-based control for agents with double integrator dynamics is not sufficient to achieve the formation maintenance problem and further modifications are needed.

Consider a system of n ($n \geq 2$) agents, moving in a 2-dimensional Euclidean space. The agents can be modeled as single integrators, i.e.,

$$\dot{x}_i(t) = u_i(t), \quad i = 1, \ldots, n, \tag{3.1}$$

or as double integrators,

$$\begin{aligned} \dot{x}_i(t) &= v_i(t) \\ \dot{v}_i(t) &= u_i(t), \end{aligned} \tag{3.2}$$

where $x_i(t) \in \mathbb{R}^2$ and $v_i(t) \in \mathbb{R}^2$ are the coordinates vector and the velocity vector assigned to the i-th agent correspondingly. $u_i(t) \in \mathbb{R}^2$ denotes the control input associated with that agent.

Agents can communicate with each other in various ways and are able to collect data such as relative measurements (i.e., distances and relative-positions). Graph theory has emerged as the correct mathematical tool for modeling pairwise relations between agents. In terms of graph

© Technion - Israel Institute of Technology, Elyachar Central Library

theory, the agents are modeled as nodes and the associated communication methods as edges of graph $\mathcal{G}$. Also, we consider the graph to be undirected, meaning that there is no distinction between two vertices associated with the same edge. A *formation* can be defined by specifying the distances between pairs of agents in the system. Denote d_k as the desired distance between agent i and j for edge number k,[1] $(i,j) \in \mathcal{E}$, and let $d = \begin{bmatrix} d_1^2 & \cdots & d_m^2 \end{bmatrix}^{\mathrm{T}} \in \mathbb{R}^m$ represent the *distance constraint vector*.

The *distance error*, $\delta \in \mathbb{R}^m$, is defined as the difference between the measured relative distances and the desired inter-agent distances,

$$\delta_k = \|e_k\|^2 - d_k^2, \quad k \in \{1, \dots, m\}. \tag{3.3}$$

As a first step, a control law is introduced, purposed to drive the agents in a way such that the distances between them satisfy the distances constraints that we want, i.e., the control $u_i(t)$ should result in

$$\lim_{t\to\infty} \|x_j(t) - x_i(t)\| = \lim_{t\to\infty} \|e_k(t)\| = d_k\,, \ \ \forall e_k \in \mathcal{E}, \tag{3.4}$$

where $d \in \mathbb{R}^m$ is the distance constraints vector. In terms of the distance error that was defined in (3.3), equation (3.4) may be written as:

$$\lim_{t\to\infty} \delta_k = 0\,, \ \ \forall e_k \in \mathcal{E}. \tag{3.5}$$

Consider that the actual formation of the agents is represented by the framework $\mathcal{G}(x)$, formed by the configuration $x = (x_1, \cdots, x_n) \in \mathbb{R}^{2n}$ together with the graph $\mathcal{G}$. The formation is imposed such that the resulting framework is minimally and infinitesimally rigid, hence not all the relative position measurements are required. In this direction, we first introduce the following assumption, which is widely used in the literature [15, 22], and it will accompany us throughout the thesis.

Assumption 1. *Any framework $\mathcal{G}(x)$ satisfying the distance constraints $\{d_{ij}\}_{(i,j)\in\mathcal{E}}$ is minimally infinitesimally rigid.*

3.1 Gradient Formation Control Law

In [21], the well known gradient control law is proposed to locally and asymptotically stabilize infinitesimally rigid formations. The associated positive semi-definite potential function is

[1] At times we will also write d_{ij}.

defined as

$$\Phi(e) = \frac{1}{2}\sum_{k=1}^{m}\left(\|e_k\|^2 - d_k^2\right)^2 = \frac{1}{2}\sum_{k=1}^{m}\delta_k^2. \tag{3.6}$$

Observe that $\Phi(e) = 0$ if and only if $\|e_k\|^2 = d_k^2 \;\; \forall k = 1, \ldots, m$.

The control for each agent is then taken as the gradient of the potential function (3.6),

$$u_i(t) = -\left(\frac{\partial \Phi(e)}{\partial x_i}\right) = -\sum_{j\sim i}\left(\|e_k\|^2 - {d_k}^2\right)e_k. \tag{3.7}$$

By using the control law in (3.7), it can be written in state space form by using the definition of the rigidity matrix $R(x)$ for all the agents as

$$u(t) = -R(x)^T R(x)x(t) + R(x)^{\mathrm{T}}d. \tag{3.8}$$

This control law has been proven to ensure local asymptotic stability [21, 22].

3.2 Formation Maneuvering

Formation maneuvering, where the agents are required to simultaneously acquire a formation and move cohesively following one leader, is an important task for surface and aerial vehicles. The formation's centroid and its derivatives represent the behavior and motion of the formation and are given in the following equations:

$$\bar{x} \triangleq \frac{1}{n}\left(\mathbf{1}_n^{\mathrm{T}} \otimes I_2\right)x, \tag{3.9}$$

$$\bar{v} \triangleq \dot{\bar{x}} = \frac{1}{n}\left(\mathbf{1}_n^{\mathrm{T}} \otimes I_2\right)\dot{x}, \tag{3.10}$$

$$\bar{a} \triangleq \ddot{\bar{x}} = \frac{1}{n}\left(\mathbf{1}_n^{\mathrm{T}} \otimes I_2\right)\ddot{x}. \tag{3.11}$$

Equations (3.9), (3.10) and (3.11) describe the position, velocity and acceleration of the centroid respectively. Consider the formation controller in (3.8) and designate one agent as a leader. The leader is injected with an external reference velocity command $v_{ref} \in \mathbb{R}^2$, where v_{ref} is constant. The objective of the formation is to move at the same velocity and follow the leader's reference velocity (hence, the centroid's velocity will also be the same as the reference) while maintaining the formation shape. In other words, the goal is to find a control law $u_i(t)$ that will satisfy (3.4) and also

$$\lim_{t\to\infty}\|v_i(t) - v_{rerf}\| = 0 \;\; i = 1, ..., n. \tag{3.12}$$

© Technion - Israel Institute of Technology, Elyachar Central Library

Note that $u_i(t)$ can be the velocity input or the acceleration input depending on the mathematical model.

For the first order system, without the presence of any additional control, such a scheme will always lead to a steady-state error for the formation, i.e., $\lim_{t\to\infty} \|\delta(t)\| > 0$. This phenomena is demonstrated by a simple example shown in Figure 3.1(a). Here, 4 agents with single integrator dynamics are tasked with maintaining a diamond shape formation (satisfying Assumption 1) while tracking the designated leader (marked in green). Figure 3.1(b) plots $\|\delta(t)\|$ showing the steady-state error.

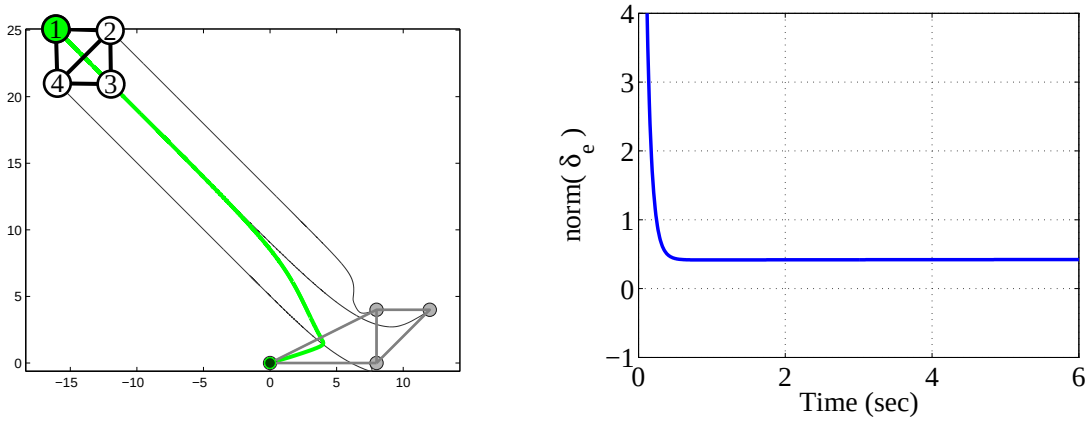

(a) An MIR formation tracking a leader.

(b) A plot of $\|\delta(t)\|$ showing a steady-state error.

Figure 3.1: Without any additional control, tracking a leader leads to a steady-state error in the formation.

The method for solving the problem for agents with single-integrator dynamics will be discussed in Chapter 4. The well known distance-constrained formation control law will be presented, as well as the derivation of the formation distance error dynamics. Then, the stability analysis of the system will be discussed, with and without a control mechanism for the dynamics with velocity reference.

As for the second order system described in (3.2), solely implementing the distance-based control law in (3.8) as the acceleration input, i.e.,

$$\begin{bmatrix} \dot{x}(t) \\ \dot{v}(t) \end{bmatrix} = \begin{bmatrix} 0 & I \\ -R(x)^T R(x) & 0 \end{bmatrix} \begin{bmatrix} x(t) \\ v(t) \end{bmatrix} + \begin{bmatrix} 0 \\ R(x)^T \end{bmatrix} d, \tag{3.13}$$

will result in a non-stable system.

In witness whereof, simulating the dynamics in (3.13) for a 6 agents system results with agents that cannot maintain the desired hexagon formation (as in Figure 3.2). The initial velocities are all zeros and the initial positions of the agents are depicted in grey circles. As can be seen from the trajectories in Figure 3.3(a), the formation is not asymptotically stable. The formation error is plotted in Figure 3.3(b) in where we can see it does not converge to zero.

© Technion - Israel Institute of Technology, Elyachar Central Library

© Technion - Israel Institute of Technology, Elyachar Central Library

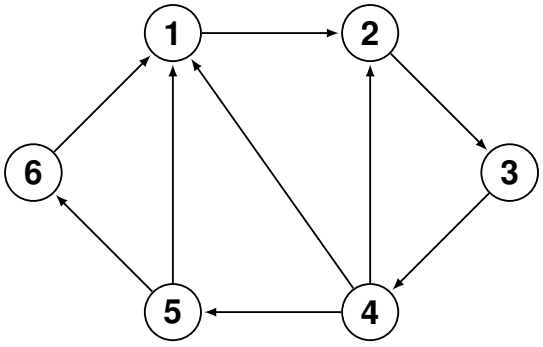

Figure 3.2: An example of a desired Hexagon shape for a 6 agents formation

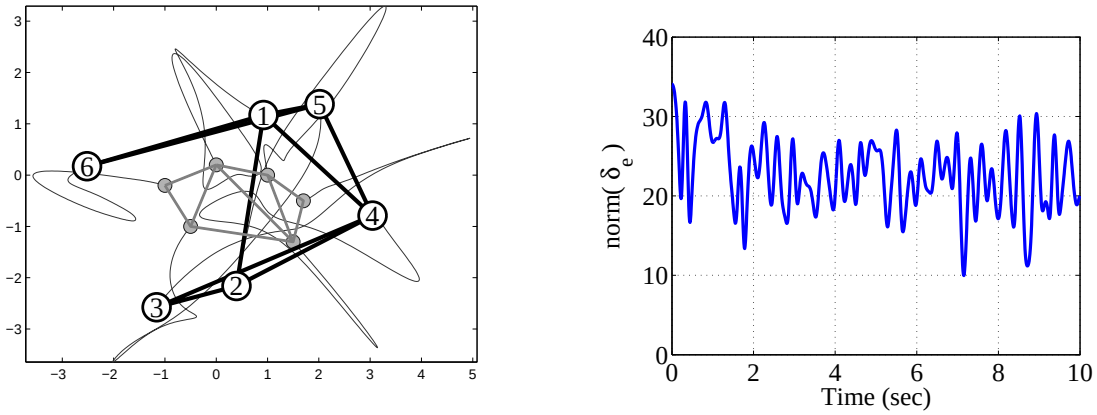

(a) Unstable MIR formation.

(b) The distance error $\|\delta(t)\|$ does not converge to 0.

Figure 3.3: Distance-based Formation control for agents with double integrator dynamics.

This phenomena for agents with double-integrator dynamics is explained and handled substantially in 5. Distance-based control combined with velocity consensus mechanism is used in order to stabilize the suitable error dynamics. At the end of that chapter, the velocity tracking problem, for a system with velocity reference as an input to a leader, is then considered and analyzed.

© Technion - Israel Institute of Technology, Elyachar Central Library

© Technion - Israel Institute of Technology, Elyachar Central Library

Chapter 4

Single-Integrator Dynamics

In this chapter we explore the formation control where each agent has single integrator dynamics. One of the chapter's contributions is to derive an associated dynamical system based on the formation error. An alternative stability proof on the error dynamics will then be provided by using Lyapunov's indirect method. We manage to connect the error properties to those of the graph and to find an upper bound for the linearized system.

When one of the agents is subjected to an external reference velocity and with the absence of any additional control action, the standard rigidity based formation stabilization solutions will exhibit a steady-state formation error. The main contribution of this chapter is the introduction of a control scheme that will enable to implement a stabilizing controller over the error in order to manipulate it. We demonstrate how the error can be decreased by using a proportional control and completely eliminated by using PI controller. A mathematical proof is also provided and simulations are given to support the results.

4.1 Distance-Constrained Formation Stabilization

The goal of this section is to introduce a controller u_i such that the terms defined by (3.4) are satisfied. Those terms are partial requirements of the main objective that was presented in Chapter 3, and aimed at acquiring distance between agents according to the distances constraints.

Consider a system of n ($n \geq 2$) agents, modeled as first-order integrators, as described in (3.1). The entire system can be written as

$$\dot{x}(t) = u(t),$$

and to simplify notations, the time variable in $x(t)$ and $u(t)$ will be omitted (i.e., $x(t) := x$).

© Technion - Israel Institute of Technology, Elyachar Central Library

4.1.1 Formation Stability Analysis

The stability analysis of the this control strategy has been investigated in many works, starting from center manifold theorem for the linearized dynamics [21] to employing Lyapunov based approaches [14, 15]. It is well known that the direct linearization of (3.8) around the target formation has multiple eigenvalues at the origin, and consequently cannot be analyzed by Lyapunov's indirect method [21]. By deriving an associated dynamical system based on the formation error for MIR framework, we show that the linearization of the error dynamics leads to a Hurwitz state matrix, and thus local asymptotic stability is readily shown.

By factorizing the dynamics in (3.8) yields

$$\dot{x}(t) = -R(x)^{\mathrm{T}} \left(R(x)x(t) - d \right). \tag{4.1}$$

From (2.1) it can be shown that the expression $R(x)x(t) - d$ is the distance error vector defined in (3.3), i.e.,

$$\delta \triangleq R(x)x(t) - d = \mathrm{diag}(e_i^{\mathrm{T}}) \underbrace{(E^{\mathrm{T}} \otimes I_2)x(t)}_{e} - d. \tag{4.2}$$

As we are concerned with the behavior of the formation error, we now derive the formation error dynamics by differentiating (4.2) with respect to time,

$$\dot{\delta} = 2\,\mathrm{diag}(e_i^{\mathrm{T}})\dot{e} = 2\,\mathrm{diag}(e_i^{\mathrm{T}})(E^{\mathrm{T}} \otimes I_2)\dot{x}. \tag{4.3}$$

Combining (2.1) , (4.1) and (4.3) yields

$$\dot{\delta} = -2R(x)R(x)^{\mathrm{T}} \underbrace{\left(R(x)x(t) - d \right)}_{\delta}. \tag{4.4}$$

Theorem 5. *Under Assumption 1, the origin of the formation error dynamics (4.4) is locally asymptotically stable.*

Proof. Define a set $\Omega = \{x |\, R(x)x - d = 0\}$. For any $x^* \in \Omega$, $\delta = 0$ by definition, hence any $x^* \in \Omega$ corresponds to an equilibrium of (4.4). Denote $M(x) = R(x)R(x)^{\mathrm{T}}$. Evaluating the Jacobian of the dynamics (4.4) at the equilibrium $\delta = 0$ ($x = x^*$) gives

$$\begin{aligned} \left.\frac{\partial f(\delta)}{\partial \delta}\right|_{\delta=0, x=x^*} &= \left.\frac{\partial \left(-2M(x)\delta\right)}{\partial \delta}\right|_{\delta=0, x=x^*} \\ &= -2\left(\frac{\partial \left(M(x)\right)}{\partial \delta}\delta\right)\Bigg|_{\delta=0, x=x^*} -2\left(M(x)\frac{\partial \delta}{\partial \delta}\right)\Bigg|_{\delta=0, x=x^*}. \end{aligned} \tag{4.5}$$

The linearized dynamics equation thus can be expressed as

$$\dot{\tilde{\delta}} = -2M(x^*)\tilde{\delta}\,, \tag{4.6}$$

where $\tilde{\delta}$ is the variation of the state around the equilibrium point.

From Assumption 1 and Corollary 1, it follows that $R(x^*)$ has full row rank, and therefore $M(x^*)$ is a symmetric positive-definite matrix. Thus, the equilibrium point $\delta = 0$ of the nonlinear formation error dynamics is locally asymptotically stable. □

The result of Theorem 5 shows that examining the linearized formation error dynamics allows for the use of Lyapunov's indirect method to show local asymptotic stabilization of the formation. In fact, exponential stability can also be shown using a similar approach as found in [15].

4.1.2 Simulations

Consider for example a 4 agents system in which each agent is implemented with a distributed control law as in (3.7). As can be seen in Figure 4.1(a), for an arbitrary initial positions (depicted in grey), the formation reaches the desired squared shape. The norm of the formation error is plotted as well in Figure 4.1(b) in order to support this result.

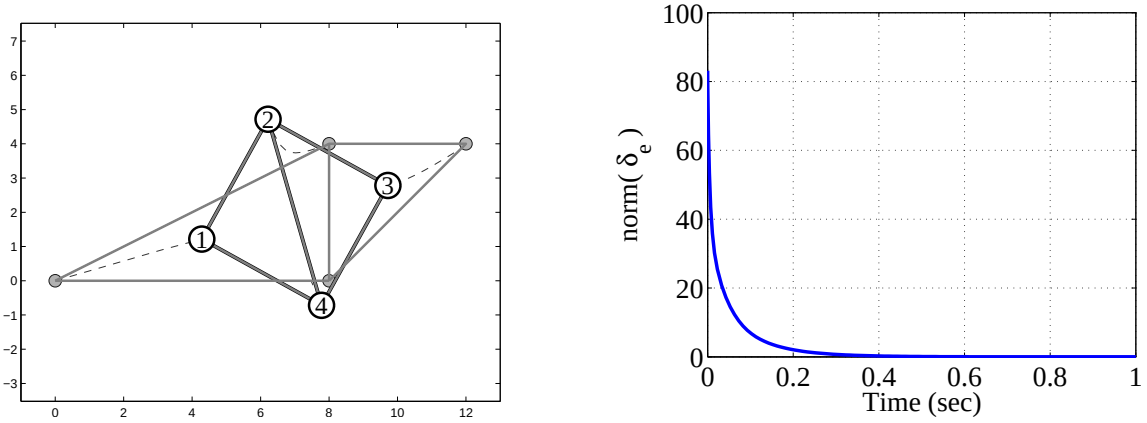

(a) Trajectories of 4 agents with a distance based control law.

(b) A plot of $\|\delta\|$ showing zero steady-state formation error.

Figure 4.1: MIR formation with a distance based control law.

4.2 Formation Control with Velocity Reference

Once the gradient-based controller has been successfully shown to asymptotically stabilize the zero-input system as described in (4.1), the leader is now additionally injected with an external

© Technion - Israel Institute of Technology, Elyachar Central Library

© Technion - Israel Institute of Technology, Elyachar Central Library

constant velocity command $v_{ref} \in \mathbb{R}^2$. The goal is to make the formation move at that velocity and follow the leader's reference velocity while maintaining the formation shape. The addition of a velocity reference to the agent designated as a leader together with the control law in (3.8) leads to the following dynamics,

$$\dot{x}(t) = -R(x)^{\mathrm{T}} \left(R(x)x(t) - d\right) + Bv_{ref}. \tag{4.7}$$

Here, $B \in \mathbb{R}^{2n\times 2}$ is used to indicate which agent in the formation may receive the external velocity reference, $v_{ref} \in \mathbb{R}^2$ (i.e., if agent i is the leader, then the ith block of B is I_2, and the remaining blocks are zero). The dynamics of the formation error vector with an external velocity reference can be derived from (4.7) as

$$\dot{\delta} \;\; = \;\; -2R(x)R(x)^T\delta + 2R(x)Bv_{ref}. \tag{4.8}$$

A general control scheme is presented in Figure 4.2 and can be described as

$$\dot{x}(t) = u(t) + Bv_{ref}, \tag{4.9}$$

$$u(t) = -R(x)^{\mathrm{T}} C\Big(R(x)x(t) - d\Big), \tag{4.10}$$

where $C\Big(R(x)x(t) - d\Big) = C(\delta)$, can be any stabilizing controller. In addition to preserving the stability of the closed-loop dynamics, the controller C should also eliminate the steady-state formation error dynamics, i.e.,

$$\lim_{t\to\infty} \|\delta(t)\| = 0.$$

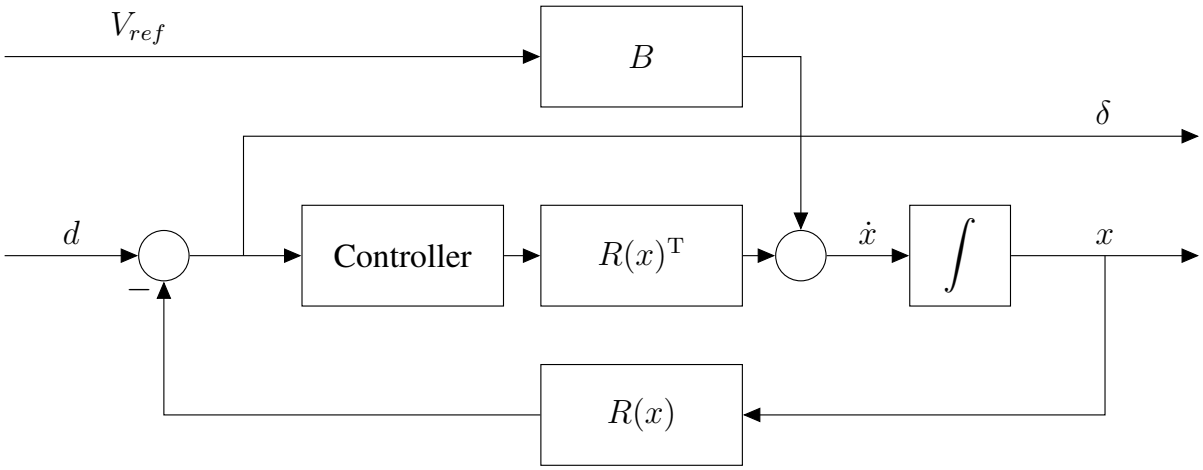

Figure 4.2: The formation control is augmented with an additional controller to eliminate the steady-state error in the formation.

Before analyzing the stability of the control scheme proposed in (4.10), we first examine

the performance of the formation with a leader. In particular, we show that for the dynamics in (4.10), assuming that C is a stabilizing controller, the velocity of the formation centroid will move at a velocity proportional to the reference, v_{ref}.

Theorem 6. *Consider the system (4.9) and (4.10) and assume C is a stabilizing controller. Then the centroid of the formation, (3.9), moves at the constant velocity v_{ref}/n.*

Proof. Observe from (2.1) that $\left(\mathbf{1}_n^{\mathrm{T}} \otimes I_2\right) R(x)^{\mathrm{T}} = \left(\mathbf{1}_n^{\mathrm{T}} \otimes I_2\right) (E \otimes I_2)\mathrm{diag}(e_i) = 0$ due to the fact that $\mathbf{1}_n$ is the left null space of E. Using this property, we examine the dynamics of the centroid,

$$\begin{aligned}\dot{\bar{x}} &= \frac{1}{n}\left(\mathbf{1}_n^{\mathrm{T}} \otimes I_2\right)\left(-R(x)^{\mathrm{T}} C(\delta) + B v_{ref}\right) \\ &= \frac{1}{n}\left(\mathbf{1}_n^{\mathrm{T}} \otimes I_2\right) B v_{ref}.\end{aligned}$$

In the case that only one agent is being controlled (i.e., $(\mathbf{1}_n^{\mathrm{T}} \otimes I_2)B = I_2$), the centroid dynamics reduce to $\dot{\bar{x}} = v_{ref}/n$, concluding the proof. □

Remark 1. *Note that the centroid does not actually track the reference velocity. However, if the number of agents in the ensemble is known by the leader, this is easily overcome by premultiplication of the reference velocity by the number of agents in the network.*

4.2.1 Proportional Gain Control

A *proportional controller* is a control loop feedback mechanism widely used in industrial control systems, and it is the first intuitive control gain that comes to mind when implementing a controller. A proportional controller generally operates with a steady-state error, sometimes referred to as droop. The next equation describes a proportional controller that may be implemented as the controller C in (4.10),

$$u = -R(x)^{\mathrm{T}}(\kappa_P I_n)\left(R(x)x - d\right), \tag{4.11}$$

where κ_P is a scalar constant. Notice here that each agent utilizes the same gain parameter.

A proportional control system amplifies the error signal to generate the control signal. The closed-loop dynamics of the system utilizing the proportional control in (4.11) is thus

$$\dot{x} = R(x)^T(\kappa_P I_n)\left(R(x)x - d\right) + B v_{ref}.$$

Examining the system from the error vector point of view will help to prove the stability of the origin. The dynamics of the formation error vector (4.2) with a proportional controller

© Technion - Israel Institute of Technology, Elyachar Central Library

described in (4.11) can be derived as

$$\dot{\delta} \;\; = f(\delta, v_{ref}) = \;\; -2\kappa_P R(x)R(x)^T\delta + 2R(x)Bv_{ref}. \tag{4.12}$$

Theorem 7. *Under Assumption 1 and for any $\kappa_P > 0$, the origin of the zero-input $(v_{ref} = 0)$ error dynamics (4.12) is locally asymptotically stable.*

Proof. By using the same method described in Theorem 5, the linearized dynamics equation can be expressed as

$$\dot{\tilde{\delta}} = -2\kappa_P M(x^*)\tilde{\delta}\,,$$

where $\tilde{\delta}$ is the variation of the state around the equilibrium point. For any choice of $\kappa_P > 0$ the matrix $-2\kappa_P M(x^*)$ is Hurwitz (Because $M(x^*)$ is a symmetric positive-definite matrix) thus leading us to the local asymptotic stability of the equilibrium point $\delta = 0$ of the nonlinear formation error dynamics. □

Theorem 8. *In the local sense, under Assumption 1, and for any $\kappa_P > 0$, the error dynamics (4.12) is bounded input bounded output (BIBO) stable.*

Proof. Since the derivative of the formation error will become zero at steady state $(\dot{\delta}_{ss}(t)) = 0)$, the linearized error dynamics algebraic equation is

$$-2R(x^*)R(x^*)^T\kappa_P\delta + 2R(x^*)Bv_{ref} = 0, \tag{4.13}$$

which in turn leads to

$$\delta_{ss}(t) = \frac{1}{\kappa_P}M(x^*)^{-1}R(x^*)Bv_{ref}. \tag{4.14}$$

Since $R(x^*)$ and $M(x^*)^{-1}$ ($M(x^*)$ is invertible since it is symmetric positive definite matrix) are constant matrices evaluated around the equilibrium, this immediately implies that for any bound input the formation error will also be bounded. The same actions are taken as in Theorem 5 in order to present the full linearized dynamics of (4.12). Define the set $\tilde{\Omega} = \{(x, v_{ref})|\, f(x, v_{ref}) = 0\}$, which represents the equilibrium set of (4.12). We are interested in linearizing the system around a zero formation error, i.e., $\delta = 0$ and hence $x = x^*$ ($x \in \Omega$ as defined in Theorem 5). In this direction, define the set $\Omega_2 = \{(x, v_{ref})|\, R(x)x - d = 0\,, f(x, v_{ref}) = 0\} \subset \tilde{\Omega}$. It then follows that any $(x, v) \in \Omega_2$ satisfies $x \in \Omega$ and $v = 0$. We now linearize our system around the point $(x^*, 0) \in \Omega_2$ to obtain the linear state space form [29]

$$\begin{aligned} \dot{\tilde{\delta}} &= \bar{A}\tilde{\delta} + \bar{B}\tilde{v} \\ y &= \bar{C}\tilde{\delta} + \bar{D}\tilde{v}, \end{aligned}$$

where $\tilde{\delta}$ is the variation of the state and $\tilde{v}$ is the variation of the input around the equilibrium

© Technion - Israel Institute of Technology, Elyachar Central Library

point. The matrix $\bar{A}$ is obtained by evaluating the Jacobian of the dynamics (4.12) at the equilibrium $\delta = 0$ ($x = x^*$) and at the nominal input $v_{ref} = 0$:

$$\begin{aligned}\bar{A} = \left.\frac{\partial f(\delta, v_{ref})}{\partial \delta}\right|_{\delta=0, x=x^*, v_{ref}=0} &= \left.\frac{\partial \left(-2\kappa_P M(x)\delta + 2R(x)Bv_{ref}\right)}{\partial \delta}\right|_{\delta=0, x=x^*, v_{ref}=0} \\ &= -2\kappa_P M(x^*) + 2\left(\frac{\partial R(x)}{\partial \delta}Bv_{ref}\right)\Bigg|_{\delta=0, x=x^*, v_{ref}=0} \\ &= -2\kappa_P M(x^*).\end{aligned}$$

The Marix $\bar{B}$ represents the control matrix, and is obtained in a similar way:

$$\bar{B} = \left.\frac{\partial f(\delta, v_{ref})}{\partial v_{ref}}\right|_{\delta=0, x=x^*, v_{ref}=0} = 2R(x^*)B.$$

The $\bar{C}$ matrix is the identity matrix reflecting the formation error vector as the output of the system with $\bar{D} = 0$. The complete linearized dynamics equation can be expressed as

$$\begin{aligned}\dot{\tilde{\delta}} &= -2\kappa_P M(x^*)\tilde{\delta} + 2R(x^*)B\tilde{v} \\ y &= \tilde{\delta}.\end{aligned} \tag{4.15}$$

For a general linear system, the transfer functions matrix between the input and the output is given according to $G(s) = \bar{C}\left(sI - \bar{A}\right)^{-1}\bar{B} + \bar{D}$ [29]. The transfer function corresponding to the linearized dynamics (4.15) is thus

$$G(s) = \left(sI_m + 2\kappa_P M(x^*)\right)^{-1} 2R(x^*)B = 2\frac{adj\left(sI_m + 2\kappa_P M(x^*)\right)}{det(sI_m + 2\kappa_P M(x^*))}R(x^*)B. \tag{4.16}$$

BIBO stability can be concluded simply by examining the poles of $G(s)$, and those are obtained by solving the characteristic equation of $-2\kappa_P M(x^*)$. By Assumption 1, $M(x^*)$ is a symmetric positive-definite matrix, and therefore all of its eigenvalues are real and positive. Therefore, for positive κ_P, all the eigenvalues of $-2\kappa_P M(x^*)$ are located on the open left half plane and hence the system is BIBO stable. □

Owing to the structure of the matrices in the linearized dynamics, we are also able to provide an analytic expression for the steady-state error and also upper bounds that are expressed in terms of properties of the system.

Corollary 2. *Given a constant reference velocity* $\tilde{v} =$v *for the linearized dynamics in (4.15), the*

© Technion - Israel Institute of Technology, Elyachar Central Library

steady-state formation error is $\lim_{t\to\infty}\tilde{\delta}(t) = \tilde{\delta}_{ss} = \frac{1}{\kappa_P}M(x^*)^{-1}R(x^*)B\mathrm{v}$ *and it is bounded as*

$$\left\|\tilde{\delta}_{ss}\right\| \leq \left|\frac{1}{\kappa_P}\right| \frac{\sqrt{d_{max}\cdot\lambda_{max}(L(\mathcal{G}))}}{\lambda_{min}(M(x^*))}\left\|\mathrm{v}\right\|.$$

Proof. For a step input response of magnitude v we can use the final value theorem, since the eigenvalues of the dynamic matrix are all in the open left-half of the complex plane.

$$\begin{aligned}\lim_{t\to\infty}\tilde{\delta}(t) &= \lim_{s\to 0}\delta(s) = \lim_{s\to 0} s\frac{1}{s}G(s)\mathrm{v}\\ &= \lim_{s\to 0}\left(sI_m + 2M(x^*)\kappa_P\right)^{-1}2R(x^*)B\mathrm{v}\\ &= \frac{1}{\kappa_P}M(x^*)^{-1}R(x^*)B\mathrm{v}.\end{aligned}$$

Since $R(x^*)$ and $M(x^*)^{-1}$ are constant matrices, this immediately implies that for any bounded input the formation error will also be bounded. The euclidean norm of the formation error vector is considered in order to express the boundness of the steady-state error with the following norm inequality

$$\left\|\tilde{\delta}_{ss}\right\| = \left\|\frac{1}{\kappa_P}M(x^*)^{-1}R(x^*)B\mathrm{v}\right\| \leq \left|\frac{1}{\kappa_P}\right|\left\|M(x^*)^{-1}\right\|\left\|R(x^*)\right\|\left\|B\right\|\left\|\mathrm{v}\right\|. \tag{4.17}$$

From the definition of B in (4.7), its norm is $\|B\| = 1$ and hence assigning a different agent with a reference velocity does not affect the boundness of the steady state error. Also observe that

$$\begin{aligned}\|M(x^*)\| &= \left\|R(x^*)R(x^*)^T\right\|\\ &= \left\|diag(e_i^{T*})(E^T\otimes I)(E\otimes I)diag(e_i^*)\right\|\\ &\leq \left\|diag(e_i^{T*})\right\|\left\|(E^TE\otimes I)\right\|\left\|diag(e_i^*)\right\|.\end{aligned} \tag{4.18}$$

The expression E^TE is also known as $L_e(G)$, the edge Laplacian of a graph [51]. Using an SVD decomposition, the following equations hold,

$$\begin{aligned}\|E\| &= \sqrt{\lambda_{max}(E^TE)} = \sqrt{\lambda_{max}(L_e(\mathcal{G}))}\\ &= \sqrt{\lambda_{max}(EE^T)} = \sqrt{\lambda_{max}(L(\mathcal{G}))}\\ &= \left\|E^T\right\|.\end{aligned} \tag{4.19}$$

© Technion - Israel Institute of Technology, Elyachar Central Library

From the properties of the Kronecker product, the norm $\left\|(E^TE \otimes I)\right\| = \left(\left\|E^TE\right\| \cdot \|I\|\right)$, and hence $\left\|(E^TE \otimes I)\right\| = \|L_e(\mathcal{G})\|$. From (4.19) and since $L_e(\mathcal{G})$ is symmetric,

$$\|L_e(\mathcal{G})\| = \|L(\mathcal{G})\| = \lambda_{max}(L(\mathcal{G})). \tag{4.20}$$

Note also that

$$\begin{aligned}
\left\|diag(e_i^{T*})\right\| &= \|diag(e_i^*)\| \\
&= \sqrt{\lambda_{max}\left[diag(e_i^{T*})\right]\left[diag(e_i^*)\right]} \\
&= \sqrt{\lambda_{max}\begin{bmatrix} \|e_1^*\|^2 & & \\ & \ddots & \\ & & \|e_m^*\|^2 \end{bmatrix}} \\
&= \sqrt{\max_k(d_k^2)} \triangleq d_{max},
\end{aligned} \tag{4.21}$$

where $\max_k(d_k^2)$ is the largest entry of the distance constraint vector d. From (4.18), (4.20) and (4.21) the upper bound of $\|M(x^*)\|$ is

$$\|M(x^*)\| \leq d_{max} \cdot \lambda_{max}(L(\mathcal{G})), \tag{4.22}$$

and as can be seen $\|M(x^*)\|$ depends on the structure of the graph. The matrix $M(x^*)$ is symmetric and hence $\|M(x^*)\| = \lambda_{max}(M(x^*))$. This fact will help us derive an upper bound to the norm of $R(x^*)$;

$$\|R(x^*)\| = \sqrt{\lambda_{max}\left[R(x^*)R(x^*)^T\right]} = \sqrt{\lambda_{max}M(x^*)} = \sqrt{\|M(x^*)\|}. \tag{4.23}$$

Combining (4.22) with (4.23) it can be concluded that

$$\|R(x^*)\| \leq \sqrt{d_{max} \cdot \lambda_{max}(L(\mathcal{G}))}. \tag{4.24}$$

Lastly, $\|M(x^*)^{-1}\|$ should also be bounded in order to completely bound the steady state error. The norm of the inverse of a matrix is related to its condition number. Denote $\gamma(M(x^*))$ as the condition number of a matrix $M(x^*)$, i.e., $\gamma(M(x^*)) = \frac{\lambda_{max}(M(x^*))}{\lambda_{min}(M(x^*))}$. By definition, $\gamma(M(x^*)) = \|M(x^*)\| \cdot \|M(x^*)^{-1}\|$, and hence

$$\left\|M(x^*)^{-1}\right\| = \frac{\lambda_{max}(M(x^*))}{\|M(x^*)\|\,\lambda_{min}(M(x^*))} = \frac{1}{\lambda_{min}(M(x^*))}. \tag{4.25}$$

© Technion - Israel Institute of Technology, Elyachar Central Library

By collecting (4.17), (4.24) and (4.25) the steady-state error can be bounded as

$$\left\|\tilde{\delta}_{ss}\right\| \leq \left|\frac{1}{\kappa_P}\right| \frac{\sqrt{d_{max} \cdot \lambda_{max}(L(\mathcal{G}))}}{\lambda_{min}(M(x^*))} \left\|\mathrm{v}\right\|, \tag{4.26}$$

and is affected both from properties of the structure of the graph, and from the largest entry of the distance constraint vector. □

Note that the value of the steady state error is found only in the local sense, and it is not the real steady state value but rather an approximation. This is due to the fact that the matrices $R(x^*)$ and $M(x^*)^{-1}$ are computed around the equilibrium points, which accure when δ is strictly zero.

While Theorem 7 provides us with information about the stability of the autonomous system with a positive κ_P, here an additional condition on κ_P is provided in the context of error boundness. Explicitly, the upper bound will become smaller as κ_P gets larger. Keep in mind that all that glitters is not gold and that high gains have their own drawbacks. High proportional gains usually increase the maximum overshoot of the system and create a longer settling time. They also directly amplify process noise and hence increase the sensitivity to noise. Moreover, when the plant has a more complicated dynamics other than single-integrators, large gain values can lead to system instabilities (depends on the location of the system's poles and zeros).

Some graph features affect the results of this section directly or indirectly. Firstly, for a constant reference velocity, the centroid moves at a constant velocity proportional to the number of the agents in a graph. Secondly, the steady state error has an upper bound related directly to the Laplacian eigenvalues. The location of the those eigenvalues can be correlated to the graph structure, and therefore used to identify desirable and undesirable formation interconnection topologies.

By introducing a stabilizing proportional gain controller into the formation control scheme we were able to accomplish the task of reducing the formation tracking error. That task does not fully meet the requirements of the main objective described in Chapter 3. There is a need to find a more efficient controller in order to completely eliminate the steady-state error. The PI controller qualifies for that task and will be discussed broadly in the next section.

Simulations

We now demonstrate the results of Theorem 8 and Corollary 2 with a numerical example. Consider two minimally infinitesimally rigid frameworks with 6 agents as illustrated in Figure 4.3. The graph in Figure 4.3(a) has $\lambda_{max}(L(\mathcal{G})) = 6$ while the graph in Figure 4.3(b) has $\lambda_{max}(L(\mathcal{G})) = 5.343$. In order to know how the steady state error is affected by different types of graphs, the mobile agents are driven by the dynamics in (4.9) under control law (4.11) and

© Technion - Israel Institute of Technology, Elyachar Central Library

© Technion - Israel Institute of Technology, Elyachar Central Library

are initialized with arbitrary positions and zero velocities. We would expect a graph with a lower $\lambda_{max}(L(\mathcal{G}))$ to yield a smaller upper bound, according to Corollary 2.

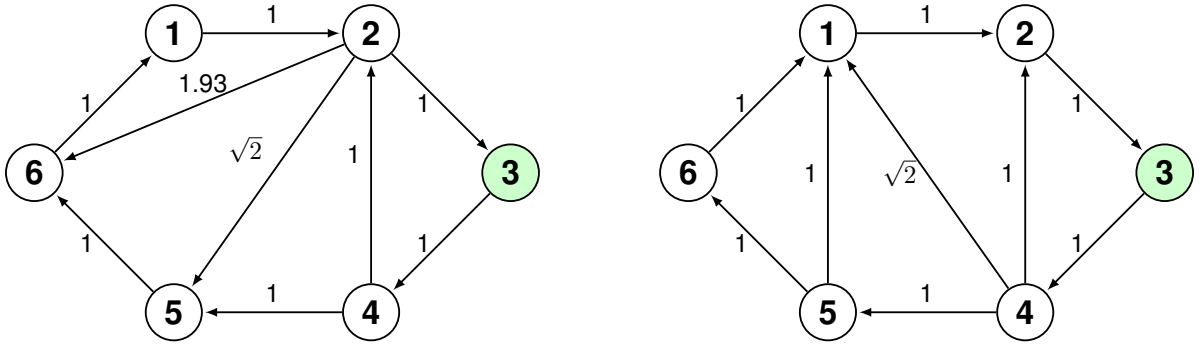

(a) Graph 1. (b) Graph 2.

Figure 4.3: The distance constraint vector d as it is presented graphically on a two types of graphs.

The desired inter-agents distances were chosen such that the target formation will have the same geometric shape, and are labeled above the edges of each graph in Figure 4.3. Also, only the green colored agent is injected with a reference velocity, with a magnitude of $0.2[m/sec]$.

The motion of the agents is illustrated in Figure 4.4 in which the initial positions are marked with grey circles and the final positions (at t_{final}) with numbered circles. The dashed lines are the trajectories of each agent and the proportional controller gain was initially set to $\kappa_P = 2$.

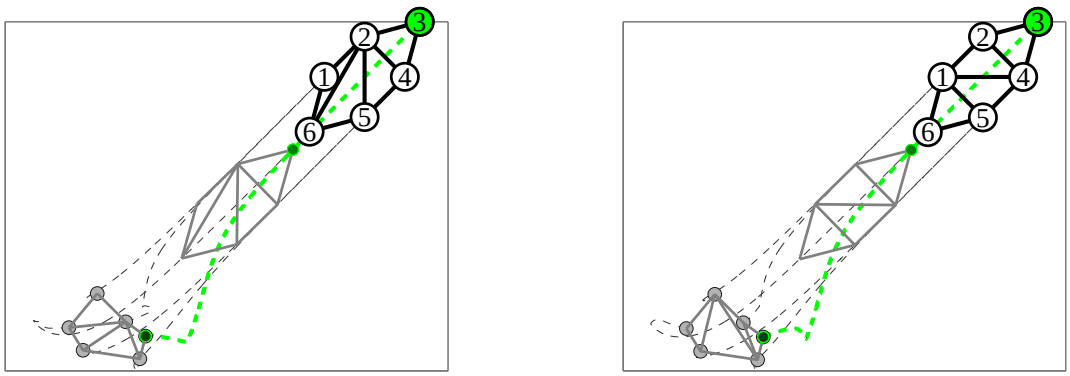

(a) Agents trajectories according to Figure 4.3(a). (b) Agents trajectories according to Figure 4.3(b).

Figure 4.4: A MIR formations tracking a leader.

Figure 4.5 describes the norm of the true error, δ. It can be seen that the steady state error indeed closely matches the linearized steady state value, marked in a green dashed line, as it is derived from (4.17). As a comparison, the true steady state value of Figure 4.5(a) is $\delta_{ss} = 0.0411$ while the steady state value from Figure 4.5(b) is $\delta_{ss} = 0.0418$. Sharp-eyed readers may see that although the bound for Graph 2 (in Figure 4.4(b)) is smaller than that for

Graph 1 (in Figure 4.4(a)), the simulation actually shows a smaller steady state error for Graph 1. That is due to the fact that the bound is not tight and is only an approximation which was derived from the linearized version of the non-linear system.

In line with the expectations, smaller $\lambda_{max}(L(\mathcal{G}))$ does cause the upper bound to be smaller, but this does not promise us that is how it will be for other types of graphs. The combination of $\lambda_{max}(L(\mathcal{G}))$, $\lambda_{min}(M(x^*))$, and d_{max} should be considered as a whole in order to examine this bound accurately. In this example the framework in Figure 4.4(a) has $\lambda_{min}(M(x^*)) = 0.57$ and the framework in 4.4(b) holds $\lambda_{min}(M(x^*)) = 1.996$ which according to Corollary 2 affirms the correctness of the results. Lastly, as κ_P increases, the steady state formation error gets smaller. This can be observed by the norm of the error for different values of κ_P in Figure 4.6.

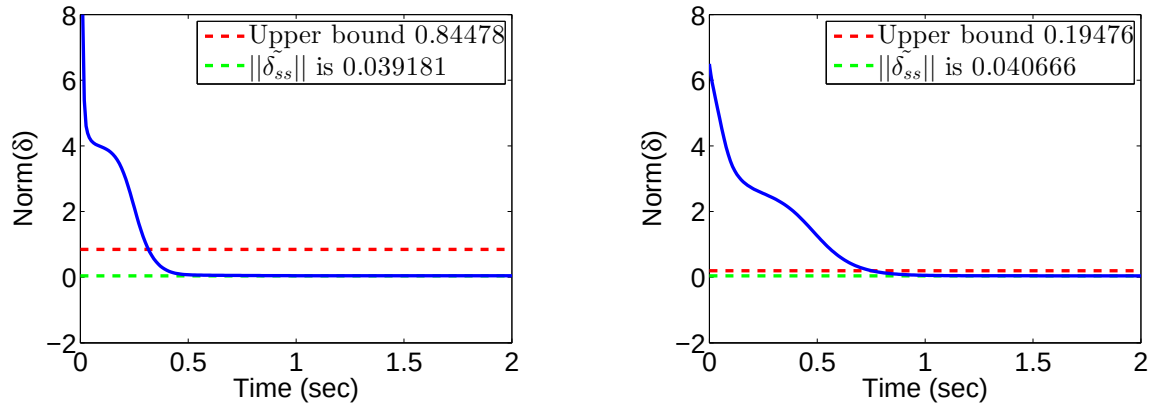

(a) The formation error norm, $\|\delta\|$, in correspondence to the formation in Figure 4.3(a).

(b) The formation error norm, $\|\delta\|$, in correspondence to the formation in Figure 4.3(b).

Figure 4.5: The norm of the formation tracking error with an upper bound

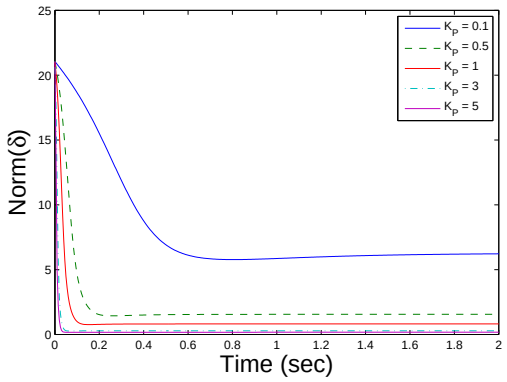

Figure 4.6: Norm of the formation error for different κ_P gain values.

© Technion - Israel Institute of Technology, Elyachar Central Library

© Technion - Israel Institute of Technology, Elyachar Central Library

4.2.2 Proportional Integral Control

So far we have shown that by using a proportional control we can reduce the formation error, but not eliminate is completely. By looking at the external velocity from a different perspective, we can come up with another type of control that will help us achieve this goal. The external reference velocity may be thought of as a disturbance to the system dynamics, causing a steady state error. As described extensively in the literature [4,29,38], one of the proportional integral controller capabilities is disturbances rejection. By adding an integral term, which is proportional to both the magnitude of the error and the duration of the error, we are able to eliminate the residual steady-state error that occurs with a pure proportional controller. Examining the eigenvalues of the linearized error dynamics with the PI controller will tell us that it is asymptotically stable, and simulations are presented to support this result.

The next equation describes a proportional-integrator controller that is implemented as the controller C in (4.10),

$$u(t) = -R(x)^{\mathrm{T}}\kappa_P \left(R(x)x(t) - d\right) - R(x)^{\mathrm{T}}\kappa_I \int_0^{\mathrm{T}} \left(R(x)x(\tau) - d\right) d\tau, \tag{4.27}$$

where κ_P and κ_I are scalar constants.

The integrator used in the controller introduces a new state-variable into the system,

$$\dot{\zeta} = \kappa_I \left(R(x)x(t) - d\right), \tag{4.28}$$

and by combining (4.9) with control law (4.27) the closed-loop dynamics can be expressed as

$$\begin{bmatrix} \dot{x}(t) \\ \dot{\zeta}(t) \end{bmatrix} = \begin{bmatrix} -\kappa_P R(x)^{\mathrm{T}} R(x) & -R(x)^{\mathrm{T}} \\ \kappa_I R(x) & 0 \end{bmatrix} \begin{bmatrix} x(t) \\ \zeta(t) \end{bmatrix} + \begin{bmatrix} \kappa_P R(x)^{\mathrm{T}} \\ -\kappa_I I \end{bmatrix} d + \begin{bmatrix} B \\ 0 \end{bmatrix} v_{ref}. \tag{4.29}$$

Examining the system from the error vector point of view will be helpful when discussing the stability near the origin. By a coordinate transformation as in (4.3), and by using (4.2.2), the formation error dynamics are

$$\begin{bmatrix} \dot{\delta}(t) \\ \dot{\zeta}(t) \end{bmatrix} = \begin{bmatrix} -2\kappa_P M(x) & -2M(x) \\ \kappa_I I & 0 \end{bmatrix} \begin{bmatrix} \delta(t) \\ \zeta(t) \end{bmatrix} + \begin{bmatrix} -2R(x)B \\ 0 \end{bmatrix} v_{ref}, \tag{4.30}$$

where $M(x) = R(x)R(x)^{\mathrm{T}}$.

Theorem 9. *Given that Assumption 1 holds, for any $k_P, k_I > 0$, the origin of the zero-input ($v_{ref} = 0$) error-dynamics in (4.2.2) is asymptotically stable.*

© Technion - Israel Institute of Technology, Elyachar Central Library

Proof. By following a similar procedure as in Theorem 5, we note that for any $x^* \in \Omega$, δ is zero by definition, which in turn leads to the equilibrium condition $\zeta = 0$. Hence, any $x^* \in \Omega$ corresponds to an equilibrium point. Denote

$$A(x) = \begin{bmatrix} -2\kappa_P R(x)R(x)^{\mathrm{T}} & -2R(x)R(x)^{\mathrm{T}} \\ \kappa_I I & 0 \end{bmatrix}.$$

Linearizing around $x = x^*$ gives us the linearized dynamics

$$\begin{bmatrix} \dot{\tilde{\delta}}(t) \\ \dot{\tilde{\zeta}}(t) \end{bmatrix} = \begin{bmatrix} -2\kappa_P M(x^*) & -2M(x^*) \\ \kappa_I I & 0 \end{bmatrix} \begin{bmatrix} \tilde{\delta}(t) \\ \tilde{\zeta}(t) \end{bmatrix},$$

where $M(x^*) = R(x^*)R(x^*)^{\mathrm{T}}$ as before.

By Assumption 1, $M(x^*)$ is a symmetric positive-definite matrix, and therefore all of its eigenvalues are real and positive. Denote the eigenvalues of $M(x^*)$ as μ_i. In order to learn about the location of the eigenvalues of $A(x^*)$, we need to solve its characteristic equation. The following lemma will be useful for the analysis.

Lemma 2. *([9])*

The determinant of a block matrix $A = \begin{bmatrix} A_{11} & A_{12} \\ A_{21} & A_{22} \end{bmatrix}$ *is given by the formula*

$$|A| = |A_{22}| \left| A_{11} - A_{12}A_{22}^{-1}A_{21} \right| . \tag{4.31}$$

From Lemma 2, the characteristic polynomial of $A(x^*)$ is thus

$$\begin{aligned} |\lambda I - A(x^*)| &= |\lambda I| \left| \lambda I + 2\kappa_P M(x^*) + \frac{2}{\lambda} k_I M(x^*) \right| \\ &= \left| \lambda^2 I + (2\kappa_P \lambda + 2\kappa_I) M(x^*) \right| . \end{aligned}$$

Since $M(x^*)$ is symmetric, it is also diagonalizable, i.e., there exists a matrix Q such that $M(x^*) = Q^{-1}DQ$, where $D = \mathrm{diag}(\mu_i)$. Hence, the characteristic polynomial can be written as

$$\begin{aligned} |\lambda I - A(x^*)| &= \left| \lambda^2 Q^{-1}Q + (2\kappa_P \lambda + 2\kappa_I) Q^{-1}DQ \right| \\ &= \left| \lambda^2 I + (2\kappa_P \lambda + 2\kappa_I) D \right| \\ &= \prod_{i=1}^{m} \left(\lambda^2 + (2\kappa_P \lambda + 2\kappa_I) \mu_i \right) . \end{aligned}$$

The ith eigenvalue of $A(x)$ can be computed as

$$\lambda_i = \frac{-2\kappa_P\mu_i \pm \sqrt{4\left(\kappa_P\mu_i\right)^2 - 8\kappa_I\mu_i}}{2}. \tag{4.32}$$

Since $\mu_i > 0$ is positive, it follows that κ_p must be positive in order for the real part of λ_i to be in the open left-half plane. Furthermore, for positive κ_I, all the eigenvalues must also be in the left-half plane. Therefore, for any $\kappa_p, \kappa_I > 0$, by Lyapunov's indirect method, we conclude that the zero-input $(v_{ref} = 0)$ error-dynamics in (4.2.2) is asymptotically stable at the equilibrium point $\delta = 0, \zeta = 0$. □

Simulations

We now demonstrate the results of Theorem 9 with a numerical example. Consider a group of 6 mobile agents implementing the PI formation controller (4.2.2). A single leader is injected with a reference velocity forming a circle. The resulting trajectories are shown in Figure 4.7(a); the initial positions are depicted in grey and the leader is labeled by the green node. All of the agents have zero initial velocities. A value of $\kappa_P = 2$ and $\kappa_I = 3$ were used for the control. As shown in Figure 4.7(b), the PI controller leads to a zero steady-state error for the formation. However, since the integral term responds to accumulated errors from the past, it can cause the present value to overshoot the setpoint value or cause oscillations to the error.

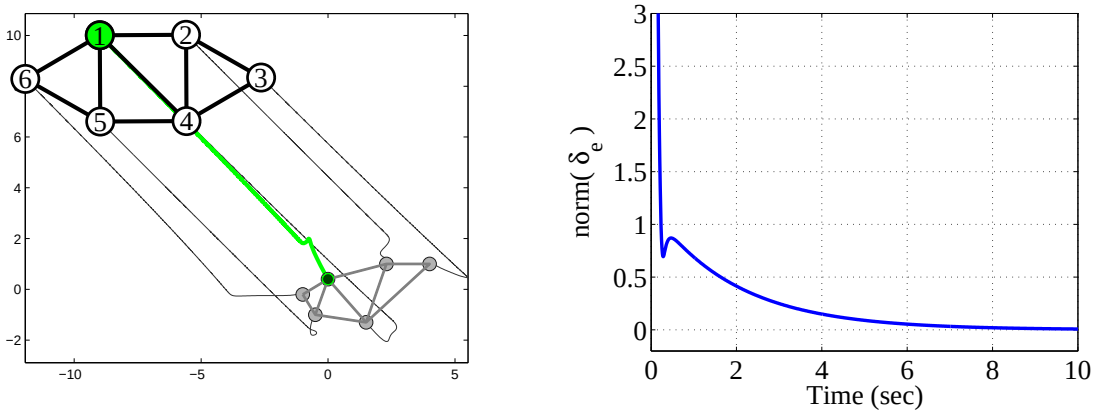

(a) An MIR formation tracking a leader with a PI controller.

(b) The steady-state error $\|\delta(t)\|$ asymptotically converges to 0.

Figure 4.7: PI Formation control with velocity reference.

It is in our interest to verify that the PI controller can handle slowly time varying disturbances. As described in Figure 4.8(a), the green leader is injected with a sinusoidal reference velocity and the remaining agents have to follow it while maintaining the pre-defined inter-

© Technion - Israel Institute of Technology, Elyachar Central Library

agents distances. Indeed, as shown in Figure 4.8(b), the PI controller does a really good job to reject those disturbances.

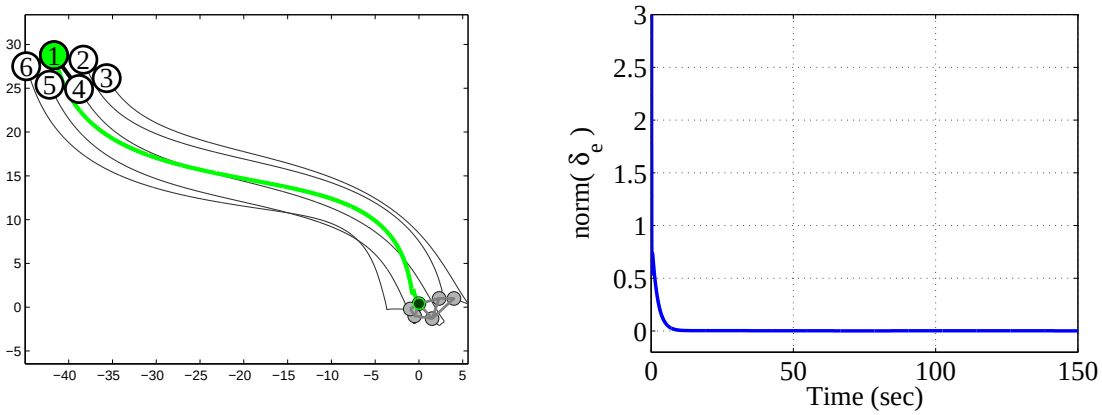

(a) An MIR formation with a PI controller tracking a leader with slow time varying reference velocity.

(b) The PI controller leads to a satisfactory small error $\|\delta(t)\|$.

Figure 4.8: PI Formation control with time varying velocity reference.

© Technion - Israel Institute of Technology, Elyachar Central Library

© Technion - Israel Institute of Technology, Elyachar Central Library

Chapter 5

Double-Integrator Dynamics

In this chapter, we extend our discussion to a second order system with agents having a double integrator dynamics where the goal is for the agents to acquire and maintain a predefined shape in the plane. Secondly, the agents are required to simultaneously acquire a formation and move cohesively following an agent with external velocity reference. For that purpose a rigidity-based control law is applied along with a velocity tracking mechanism.

Similarly to the previous chapter, we first show that the centroid of the formation moves in a constant velocity, which is determined by the initial velocities of the agents. Then we derive an associated dynamical system based on the formation error, which now comprises the distance error vector and the velocities error vector. We then provide a local stability proof for the error dynamics by using Lyapunov's direct method.

5.1 Distance-Constrained Formation Stabilization

The goal of this section is to introduce a controller u_i such that the terms defined by (3.4) in Chapter 3 are satisfied. It will be shown that formation acquisition requires additional velocity feedback based on the Laplacian consensus dynamics. Consider a system of n ($n \geq 2$) kinematic point masses (also refer to as agents), moving in a 2-dimensional Euclidean space. The motion of each agent is modeled as second-order integrator,

$$\begin{bmatrix} \dot{x}_i(t) \\ \dot{v}_i(t) \end{bmatrix} = \begin{bmatrix} 0 & I_2 \\ 0 & 0 \end{bmatrix} \begin{bmatrix} x_i(t) \\ v_i(t) \end{bmatrix} + \begin{bmatrix} 0 \\ I_2 \end{bmatrix} u_i(t), \tag{5.1}$$

where $x_i(t), v_i(t) \in \mathbb{R}^2$ are the position and velocity of the i-th robot respectively and $u_i(t) \in \mathbb{R}^2$ denotes the control input.

As the objective is to find a control law that will cause the agents to maintain a predefined shape, the distance-based control law in (3.7) is solely implemented as the acceleration input:

$$\begin{bmatrix} \dot{x}(t) \\ \dot{v}(t) \end{bmatrix} = \begin{bmatrix} 0 & I \\ -R(x)^T R(x) & 0 \end{bmatrix} \begin{bmatrix} x(t) \\ v(t) \end{bmatrix} + \begin{bmatrix} 0 \\ R(x)^T \end{bmatrix} d. \tag{5.2}$$

As can be seen from the problem statement simulations in Chapter 3, that describes the dynamics in (5.2) for a 6 agents system, we see a phenomena where the agents cannot maintain the desired hexagon formation (as in Figure 3.3(a)).

This phenomena can be easily explained by looking at the dynamics of the system when the formation error is zero. At a specific point of time, t_0, although the agents have reached the desired formation, their velocities, $v(t_0)$, are not necessarily zero. They will keep on moving, breaking the formation over and over again. In contrast to the first order system, the acceleration will instantaneously become zero and not the agent's velocity.

In order to overcome this problem, a new control law is proposed that causes the distance error vector to converge to zero and also ensures that the velocities will reach consensus. This control law is based both on a gradient control law that was proposed in (3.7) and on the Laplacian consesus dynamics. The latter describes dynamics that is implemented with a distributed control law that drives the states from their initial condition to a consensus, and conserves the sum of the initial states [25, 41]. Each agent implements the following control law:

$$u_i(t) = -\sum_{j\sim i} \left(\|e_k\|^2 - {d_k}^2 \right) e_k - \sum_{j\sim i} \left(v_j - v_i \right). \tag{5.3}$$

A scheme for the closed loop dynamics is presented in Figure 5.1 and is written in state space form as:

$$\begin{bmatrix} \dot{x}(t) \\ \dot{v}(t) \end{bmatrix} = \begin{bmatrix} 0 & I_{2n} \\ -R(x)^T R(x) & -(L \otimes I_2) \end{bmatrix} \begin{bmatrix} x(t) \\ v(t) \end{bmatrix} + \begin{bmatrix} 0 \\ R(x)^T \end{bmatrix} d \tag{5.4}$$

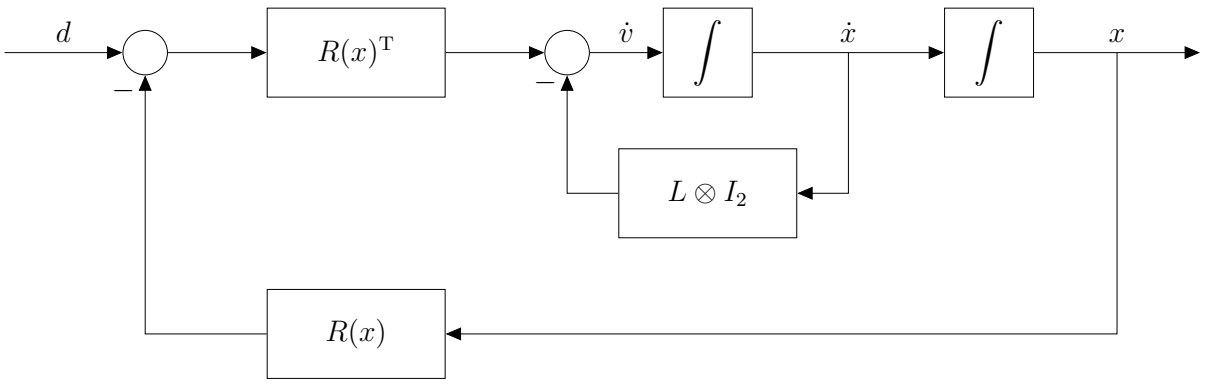

Figure 5.1: A formation control for a second order system is augmented with a velocity controller to ensure velocities consensus.

© Technion - Israel Institute of Technology, Elyachar Central Library

© Technion - Israel Institute of Technology, Elyachar Central Library

As a first step, the performance of the centroid under the implementation of the new control law is examined by the next theorem.

Theorem 10. *Consider the system (5.1) with the control law in (5.3). Then the centroid of the formation, (3.9), moves at the constant velocity* $\frac{1}{n}\left(\mathbf{1}_n^{\mathrm{T}} \otimes I_2\right) v(0)$*, which is the initial velocities average.*

Proof. The velocity of the centroid is given in the following equation by introducing the double integrator system (5.1) into (3.9):

$$\bar{v}(t) = \dot{\bar{x}}(t) = \frac{1}{n}\sum_{i=1}^{n} \dot{x}_i(t) = \frac{1}{n}\left(\mathbf{1}_n^{\mathrm{T}} \otimes I_2\right) \dot{x}(t) = \frac{1}{n}\left(\mathbf{1}_n^{\mathrm{T}} \otimes I_2\right) v(t). \tag{5.5}$$

Note that the centroid's velocity, $\bar{v} \in \mathbb{R}^2$, is the average of all agents' velocities. Observe from (2.1) that $\left(\mathbf{1}_n^{\mathrm{T}} \otimes I_2\right) R(x)^{\mathrm{T}} = \left(\mathbf{1}_n^{\mathrm{T}} \otimes I_2\right)(E \otimes I_2)\mathrm{diag}(e_i) = 0$ due to the fact that $\mathbf{1}_n$ is in the left null space of E. The same applies for $\left(\mathbf{1}_n^{\mathrm{T}} \otimes I_2\right)(L \otimes I_2) = \left(\mathbf{1}_n^{\mathrm{T}} \otimes I_2\right)(E \otimes I_2)(E^T \otimes I_2) = 0$, from the Laplacian definition in Section 2.2. By using those properties and (5.7), we examine the dynamics of the centroid,

$$\begin{aligned} \dot{\bar{x}} &= \bar{v} \\ \dot{\bar{v}} &= \frac{1}{n}\left(\mathbf{1}_n^{\mathrm{T}} \otimes I_2\right) \dot{v}(t) \\ &= \frac{1}{n}\left(\mathbf{1}_n^{\mathrm{T}} \otimes I_2\right)\left(-R(x)^T \delta_e - (L \otimes I)\, v\right) = 0. \end{aligned} \tag{5.6}$$

As can be seen, the centroid moves at a constant velocity, which is determined by the initial velocities of the agents, concluding the proof. □

Corollary 3. *Consider the system (5.1) with the control law in (5.3). For agents with zero initial velocities, the centroid of the formation, (3.9), is stationary.*

Proof. The corollary is a direct consequence of Theorem 10. □

In order to discuss the stability near the origin, an appropriate system's error is derived. Since the velocities consensus dynamics conserves the sum of the velocities, the error is connected to the definition of the centroid (3.9). Let $\delta_v \in \mathbb{R}^{2n}$ be the *velocities error vector*, defined as the difference between the velocity of each agent to the centroid's velocity , i.e.,

$$\delta_v = \begin{bmatrix} \vdots \\ v_i - \bar{v} \\ \vdots \end{bmatrix} = v - (\mathbf{1}_n \otimes \bar{v})\,. \tag{5.7}$$

Note that we can also write δ_v in terms of the agents' velocities by using (5.5) and (5.7):

$$\begin{aligned}\delta_v &= v - (\mathbf{1}_n \otimes I_2)\,\bar{v} \\ &= v - (\mathbf{1}_n \otimes I_2)\,\frac{1}{n}\left(\mathbf{1}_n^{\mathrm{T}} \otimes I_2\right) v \\ &= v - \frac{1}{n}\left(\mathbf{1}_n \mathbf{1}_n^{\mathrm{T}} \otimes I_2\right) v \\ &= \left[\left(I_n - \frac{1}{n}\mathbf{1}_n \mathbf{1}_n^{\mathrm{T}}\right) \otimes I_2\right] v. \end{aligned} \tag{5.8}$$

Theorem 10 has shown that the centroid's velocity is an invariant quantity. The invariance of $\bar{v} = \frac{1}{n}\left(\mathbf{1}_n^{\mathrm{T}} \otimes I_2\right) v$ gives more information on the velocities error vector. From the definition in (5.7), v can be written as:

$$v = (\mathbf{1}_n \otimes \bar{v}) + \delta_v. \tag{5.9}$$

By looking at (5.9), δ_v can be referred to as the *group velocity disagreement vector* and it reflects the velocity deviation of the agents from the centroid's velocity. The error δ_v is orthogonal to $\mathbf{1}$ and it also belongs to an $(2n-1)$ dimensional subspace (known as the *disagreement eigenspace* of $L \otimes I_2$ for a connected graph [30]) and satisfies the equation

$$\left(\mathbf{1}^T \otimes I_2\right) \delta_v = 0. \tag{5.10}$$

The last equation can be easily achieved by left multiplying (5.7) with $\left(\mathbf{1}^T \otimes I_2\right)$. This property appears to be necessary in order to prove the stability of the system.

5.1.1 Formation Stability Analysis

In this section we provide a stability analysis for the second order system in (5.4) by examining its error dynamics. By using Lyapunov's direct method the system is proven to be locally asymptotically stable. In contrast to Chapter 4 Lyapunov's indirect method does not work. The linearized state matrix has non-positive eigenvalues (zeros and negative eigenvalues), and the origin of the nonlinear error dynamics cannot be inferred as stable. In addition, the corresponding eigenvectors are also stated here to confirm this result.

As we are concerned with the behavior of the error, an augmented error vector $\Delta \in \mathbb{R}^{m+2n}$ is now defined, which comprises the *distance error* $\delta_e \in \mathbb{R}^m$, defined in (3.3), and the *velocities error vector*, $\delta_v \in \mathbb{R}^{2n}$, defined in (5.7),

$$\Delta = \begin{bmatrix} \delta_e \\ \delta_v \end{bmatrix} = \begin{bmatrix} R(x)x - d \\ v - (\mathbf{1}_n \otimes I_2)\,\bar{v} \end{bmatrix}. \tag{5.11}$$

© Technion - Israel Institute of Technology, Elyachar Central Library

The differentiation of the error (5.11) with respect to time is

$$\underbrace{\begin{bmatrix} \dot{\delta}_e \\ \dot{\delta}_v \end{bmatrix}}_{\dot{\Delta}} = \begin{bmatrix} 2\,\mathrm{diag}(e_i^{\mathrm{T}})\dot{e} \\ \dot{v} - (\mathbf{1}_n \otimes I_2)\,\dot{\bar{v}} \end{bmatrix} = \begin{bmatrix} 2\,\mathrm{diag}(e_i^{\mathrm{T}})(E^{\mathrm{T}} \otimes I_2)\dot{x} \\ -R(x)^T\,(R(x)x - d) - (L \otimes I)\,v \end{bmatrix}, \tag{5.12}$$

where the results of the right hand side can be explained by (5.6). Introducing 2 equations that will help us to rewrite (5.12) using the fact that $\mathbf{1}_n$ is in the right null space of E^T

$$2R(x)\delta_v = 2\,\mathrm{diag}(e_i^{\mathrm{T}})(E^{\mathrm{T}} \otimes I_2)\,[v - (\mathbf{1}_n \otimes I_2)\,\bar{v}] = 2R(x)v, \tag{5.13}$$

$$-(L \otimes I_2)\,\delta_v = -(E \otimes I_2)(E^{\mathrm{T}} \otimes I_2)\,[v - (\mathbf{1}_n \otimes I_2)\,\bar{v}] = -(L \otimes I_2)\,v. \tag{5.14}$$

By using (5.13 , 5.14), (5.12) becomes

$$\begin{bmatrix} \dot{\delta}_e \\ \dot{\delta}_v \end{bmatrix} = \begin{bmatrix} 2R(x)v \\ -R(x)^T\delta_e - (L \otimes I_2)\,v \end{bmatrix} = \begin{bmatrix} 2R(x)\delta_v \\ -R(x)^T\delta_e - (L \otimes I_2)\,\delta_v \end{bmatrix}, \tag{5.15}$$

and can be represented as an autonomous system for the error:

$$\begin{bmatrix} \dot{\delta}_e \\ \dot{\delta}_v \end{bmatrix} = \underbrace{\begin{bmatrix} 0 & 2R(x) \\ -R(x)^T & -(L \otimes I_2) \end{bmatrix}}_{A(x)} \begin{bmatrix} \delta_e \\ \delta_v \end{bmatrix}. \tag{5.16}$$

Also note that the control law (5.3) can be written in terms of the error vector by using (5.14),

$$\begin{aligned} u &= -R(x)^T R(x) + R(x)^T d - (L \otimes I)\,v \\ &= -R(x)^T\delta_e - (L \otimes I)\,\delta_v. \end{aligned} \tag{5.17}$$

As in the previous chapter, we use Assumption 1 in order to check stability by linearizing the system around an equilibrium of an MIR framework.

To correlate the states to the errors we define the set

$$\Omega_2 = \{(x, v)\,|R(x)x - d = 0, (\mathbf{1}_n \otimes I_2)\,\bar{v} - v = 0\}\,.$$

For any $(x^*, v^*) \in \Omega_2$, $\delta_e = 0$ and $\delta_v = 0$ by definition, hence any $(x^*, v^*) \in \Omega_2$ corresponds to an equilibrium of (5.16). Again, $M(x)$ is denoted as $M(x) = R(x)R(x)^{\mathrm{T}}$. Evaluating the Jacobian of the dynamics (5.16) at the equilibrium $\Delta = 0$ ($x = x^*, v = v^*$) gives

© Technion - Israel Institute of Technology, Elyachar Central Library

$$\frac{\partial\left(A(x)\Delta\right)}{\partial\Delta}\bigg|_{\Delta=0,(x,v)=(x^*,v^*)}=\left(\frac{\partial\left(A(x)\right)}{\partial\Delta}\Delta\right)\bigg|_{\Delta=0,(x,v)=(x^*,v^*)}+\left(A(x)\frac{\partial\Delta}{\partial\Delta}\right)\bigg|_{\Delta=0,(x,v)=(x^*,v^*).} \tag{5.18}$$

The linearized dynamics equation thus can be expressed as

$$\dot{\tilde{\Delta}}=A(x^*)\tilde{\Delta}\,, \tag{5.19}$$

where $\tilde{\Delta}$ is the variation of the state around the equilibrium point. The explicit form for the linearized dynamics is

$$\begin{bmatrix}\dot{\tilde{\delta}}_e\\ \dot{\tilde{\delta}}_v\end{bmatrix}=\begin{bmatrix}0 & 2R(x^*)\\ -R(x^*)^T & -\left(L\otimes I_2\right)\end{bmatrix}\begin{bmatrix}\tilde{\delta}_e\\ \tilde{\delta}_v\end{bmatrix}, \tag{5.20}$$

and it allows for a more transparent understanding of the eigenvalues. The next theorem explains why linearization can not be used to infer stability.

Theorem 11. *The matrix $A(x^*)$, which describes the linearized error dynamics (5.20) around the equilibrium, has at least three eigenvalues at the origin.*

Proof. One way of showing that $A\left(x^*\right)$ has eigenvalues at the origin is to find an eigenvector that corresponds to the zero eigenvalue. Define $u_1\in\mathbb{R}^{2n}$ and $u_2\in\mathbb{R}^{2n}$ as $u_1=\left(\mathbf{1}_n\otimes\begin{bmatrix}1 & 0\end{bmatrix}^T\right)$ and $u_2=\left(\mathbf{1}_n\otimes\begin{bmatrix}0 & 1\end{bmatrix}^T\right)$ correspondingly and recall that $\mathbf{1}_n$ belongs to the right null space of $R(x)$ and to the right null space L. Each one of them relates to a translation of the framework in a different direction [50]. The use of the kronecker product allows us to write:

$$\begin{aligned}\left(L\otimes I_2\right)u_1 &= 0\\ \left(L\otimes I_2\right)u_2 &= 0,\end{aligned} \tag{5.21}$$

and hence $\begin{bmatrix}0_m & u_1^T\end{bmatrix}^T$ and $\begin{bmatrix}0_m & u_2^T\end{bmatrix}^T$ are both eigenvectors of $A(x^*)$ that lead to a zero eigenvalue. There is also a third eigenvalue of the rigidity matrix with a corresponding zero eigenvalue, that relates to a rotation of the framework [50]. Define the position vector $\hat{x}_i\in\mathbb{R}^2$ as a permutation on the position vector of agent i such that

$$\hat{x}_i=\begin{bmatrix}0 & 1\\ -1 & 0\end{bmatrix}x_i. \tag{5.22}$$

© Technion - Israel Institute of Technology, Elyachar Central Library

© Technion - Israel Institute of Technology, Elyachar Central Library

Furthermore, define the vector $u_3 \in \mathbb{R}^{2n}$ as

$$u_3 = \begin{bmatrix} \hat{x}_1^T & \cdots & \hat{x}_n^T \end{bmatrix}^T. \tag{5.23}$$

It can now be verified that from this construction that

$$R(x^*)u_3 = 0. \tag{5.24}$$

Note that u_3 does not belong to the null space of L, i.e. $(L \otimes I_2)\, u_3 \neq 0$. Denote $u_4 \in \mathbb{R}^m$ as a non zero vector in order to create the augmented eigenvector $\begin{bmatrix} u_4^T & u_3^T \end{bmatrix}^T$ of $A(x^*)$. In order to find another eigenvector that correspond to a zero eigenvalue, we need to find what u_4 is by looking at the equation:

$$R\left(x^*\right)^T u_4 - (L \otimes I_2)\, u_3 = 0. \tag{5.25}$$

To find the explicit expression for u_4 we can use the Moore-Penrose pseudoinverse of $R(x^*)^T$, since it is not a square matrix, and it is full row rank for an MIR framework:

$$u_4 = \left[R\left(x^*\right) R\left(x^*\right)^T\right]^{-1} R\left(x^*\right) (L \otimes I_2)\, u_3. \tag{5.26}$$

Thus, $\begin{bmatrix} u_4^T & u_3^T \end{bmatrix}^T$ is the third eigenvector of $A(x^*)$ corresponding with the zero eigenvalue. □

Lyapunov's Indirect Method does not deal with linearized systems that have eigenvalues at the origin and we can not infer on the stability of the system. Nevertheless, it can be shown that the nonlinear system is asymptotically stable by using Lyapunov's direct method.

Theorem 12. *Under Assumption 1, both the formation error dynamics and the velocity error dynamics (5.16) are locally asymptotically stable.*

Proof. Consider the following Lyapunov function:

$$W = \frac{1}{2}\delta_e^T \delta_e + \delta_v^T \delta_v, \tag{5.27}$$

where W is continuously differentiable in δ_e and in δ_v.

The derivative of (5.27) is

$$\begin{aligned} \dot{W} &= \delta_e^T \dot{\delta}_e + 2\delta_v^T \dot{\delta}_v \\ &= -2\delta_e^T R(x)\delta_v + 2\delta_v^T R(x)\delta_e - 2\delta_v^T (L \otimes I_2)\, \delta_v \\ &= -2\delta_v^T (L \otimes I_2)\, \delta_v \leq 0. \end{aligned} \tag{5.28}$$

Hence, the time derivative of W is negative semi-definite ($\dot{W} \leq 0$). It is not strictly negative definite because $\dot{W} = 0$ for any $\delta_v \in S$, where $S = \{\delta_v | \, (L \otimes I_2) \, \delta_v = 0\}$, irrespective of the value of δ_e. That means the origin is a stable equilibrium, but not necessarily asymptotically stable. The set S also implies a velocity consensus, i.e., $\delta_{v_1} = \delta_{v_2} = ... = \delta_{v_n}$. By using (5.10) we can conclude that the $\delta_{v_i} = 0 \; \forall i = 1...n$ and at steady state, the components of δ_v will be zero in each direction.

LaSalle's invariance principle implies that the errors converge to a set of configurations S. Furthermore, in S, $\delta_v = 0$ and $v_i = \bar{v} \; \forall i$. The velocity error dynamics is:

$$\dot{\delta_v} = R(x)^T \delta_e = 0. \tag{5.29}$$

For a MIR graphs, R is of full row rank, and δ_e must be zero in order for (5.29) to hold. The conclusion is that the trajectories will converge to the largest invariant set $\{\delta_e, \delta_v | \, \delta_v = 0 \, , \, \delta_e = 0\}$ and at least asymptotically the control goal is achieved.

□

The velocities consensus feedback control can be interpreted essentially as a PD-like controller of the system. Both describe a control mode in which a derivative section is added to the existing controller. In order to avoid effects of the sudden change in the value of the error signal, the derivative is taken from the output response of the system variable instead of the error signal. In our case, the velocities of the agents are considered to be the output response of the system.

5.1.2 Simulations

In order to demonstrate Theorem 12 and Corollary 3 consider for example a 6 agents system, in which each agent is implemented with a distributed control law as in (5.3). As can be seen in Figure 5.2(a), for an arbitrary initial positions (depicted in grey), the formation reaches the desired hexagon shape (depicted with bold lines). Furthermore, the initial velocities of the agents are all set to zero, which means that the centroid of the system remains stationary. The norm of the formation error is plotted in Figure 5.2(b) showing that there is no steady state formation error. Also, the norm of the velocity error is plotted in Figure 5.2(c) showing zero steady state error, which implies that the agents have stopped moving.

© Technion - Israel Institute of Technology, Elyachar Central Library

© Technion - Israel Institute of Technology, Elyachar Central Library

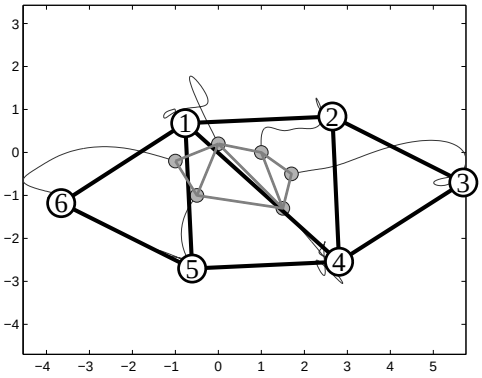

(a) An MIR formation With 6 agents.

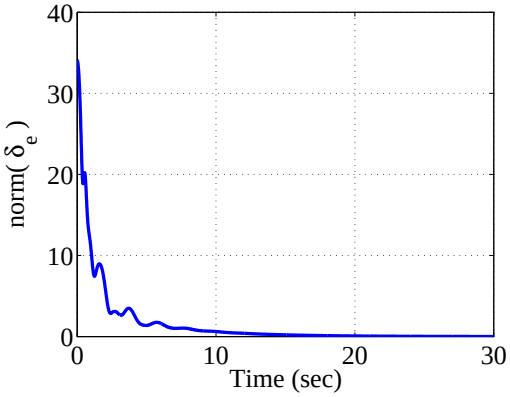

(b) A plot of $\|\delta_e(t)\|$ showing a zero steady-state distance error.

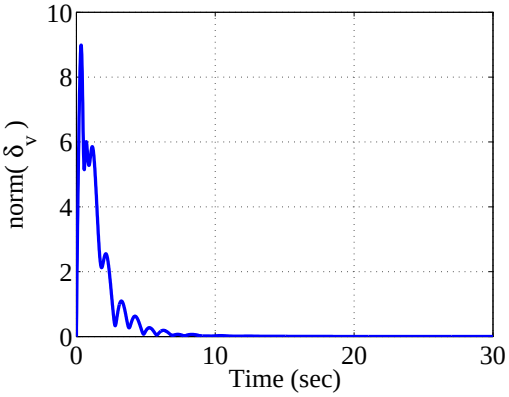

(c) A plot of $\|\delta_v(t)\|$ showing a zero steady-state velocity error.

Figure 5.2: Zero steady-state errors for MIR formation implementing control law (5.3).

In a different case, where the agents are initialized with arbitrary velocities, we expect to see the formation moving. According to Theorem 10, the velocity of the centroid is determined by the average of the initial velocities. This fact is demonstrated in Figure 5.3(a), where the same 6 agents are being initialized with

$$v_1(0) = \begin{bmatrix} 0 \\ 0 \end{bmatrix} \quad v_2(0) = \begin{bmatrix} 1 \\ 2 \end{bmatrix} \quad v_3(0) = \begin{bmatrix} -1 \\ 0 \end{bmatrix}$$
$$v_4(0) = \begin{bmatrix} -3 \\ 2 \end{bmatrix} \quad v_5(0) = \begin{bmatrix} 0 \\ 3 \end{bmatrix} \quad v_6(0) = \begin{bmatrix} -1 \\ -1 \end{bmatrix},$$

and all units are in meter per second. Calculation of the centroid's velocity yeilds

$$\bar{v} = \begin{bmatrix} -4/6 \\ 6 \end{bmatrix} \; m/sec,$$

supporting the proof.

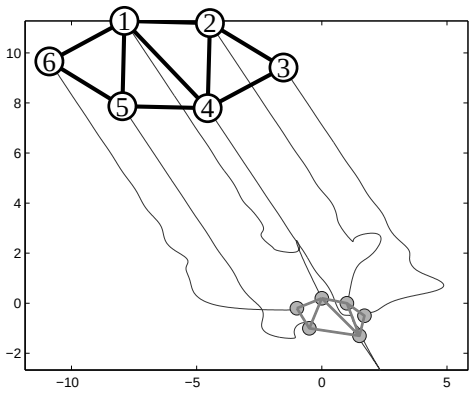

(a) An MIR formation With 6 agents.

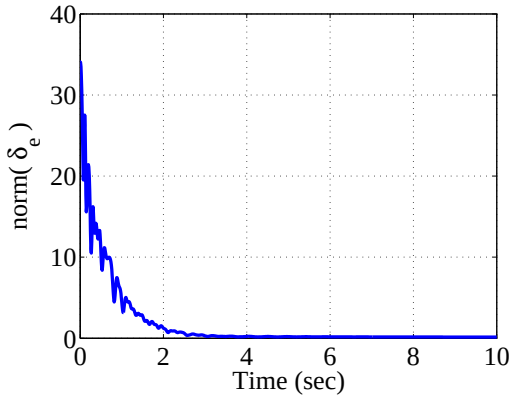

(b) A plot of $\|\delta_e(t)\|$ showing a zero steady-state distance error.

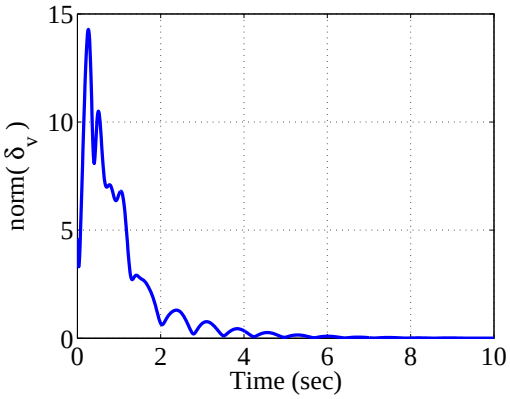

(c) A plot of $\|\delta_v(t)\|$ showing a zero steady-state velocity error.

Figure 5.3: Zero steady-state errors for MIR formation implementing control law (5.3) with arbitrary initial velocities.

5.2 Formation Control With Velocity Reference

We are interested in making the formation of the second order system, at the same manner as for the first order system, follow an external reference velocity. By injecting the reference value into the dynamics of one of the agents, we show that the centroid will follow that velocity by using an appropriate decentralized control.

Consider one agent as a leader with an external reference velocity command, as descibed in (5.30), where the objective of the formation is to follow the leader at the same velocity while

© Technion - Israel Institute of Technology, Elyachar Central Library

preserving the inter-agents distances,

$$\begin{aligned} \dot{x} &= v \\ \dot{v} &= u + Bv_{ref}, \end{aligned} \tag{5.30}$$

where $B \in \mathbb{R}^{2n\times 2}$ is used to indicate which agent in the formation may receive the external velocity reference, $v_{ref} \in \mathbb{R}^2$ (i.e., if agent i is the leader, then the ith block of B is I_2, and the remaining blocks are zero).

The addition of a velocity reference to the agent designated as a leader together with the control law in (5.4) leads to the following dynamics,

$$\begin{aligned} \dot{x} &= v \\ \dot{v} &= -R(x)^T \left(R(x)x - d\right) - \left(L \otimes I\right) v + Bv_{ref}. \end{aligned} \tag{5.31}$$

In Section 4.2 we showed that for a first order system with a reference velocity command, a steady state distance error can be overcome by using a stabilizing controller, such as a PI controller. Nevertheless, the same phenomena doesn't occur for the augmented error in the second order system and is demonstrated by a simple example shown in Figure (5.4(a)). Here, 6 agents are tasked with maintaining a hexagon shape formation (satisfying Assumption 1) while tracking the designated leader (marked in green) with a constant reference velocity. The external reference changes the equilibria of the system and without a proper stabilizing control the distances will exhibit a small steady-state error. This can be seen in Figure (5.4(b)) where the (non zero) steady-state distances error, $\|\delta_e(t)\|$, is plotted. Figure (5.4(c)) plots $\|\delta_v(t)\|$ showing that the steady-state velocity error is zero. According to the definition of δ_v in (4.2), it also means that the velocities of the agents reach a new consensus equal to the velocity of the centroid. The reason for that is because the integral action on the velocity error is obtained through the double-integrator dynamics of the agents. After closing the control loop on the velocities, the additional integrator of the dynamics reacts to the integral of the velocity error and eliminates it, similarly to a PI controller.

Before analyzing the stability of the control scheme proposed in (5.31), we first examine the performance of the formation with a leader. In particular, we show that for the dynamics in (5.31) the acceleration of the formation centroid will be proportional to the reference velocity, v_{ref}. Furthermore, we show that the ceontroid, and consequently the agents, will not follow the reference velocity and another simple feedback mechanism is needed.

Theorem 13. *Consider the system (5.31). Then for a constant reference velocity, $v_{ref} = const$, the centroid of the formation, (3.9), accelerates at a constant velocity equals to $\frac{1}{n}v_{ref}$.*

Proof. Following the same steps as in Theorem 10, the dynamics of the centroid for the system

© Technion - Israel Institute of Technology, Elyachar Central Library

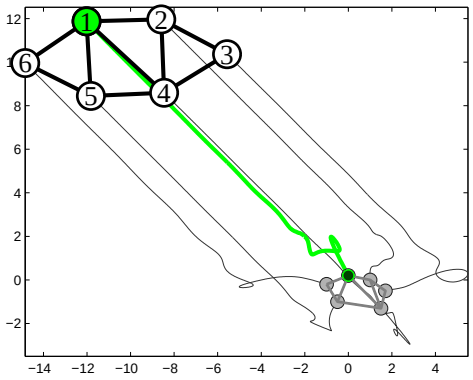

(a) An MIR formation tracking a leader.

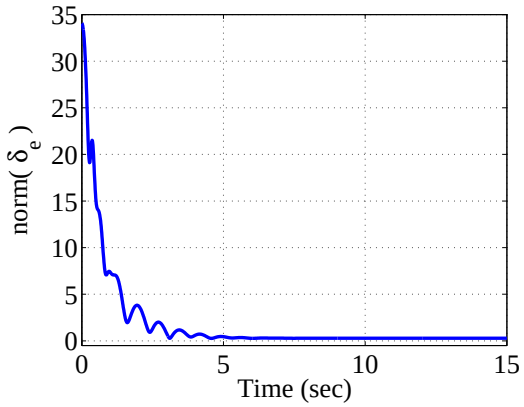

(b) A plot of $\|\delta_e(t)\|$ showing a steady-state distance error.

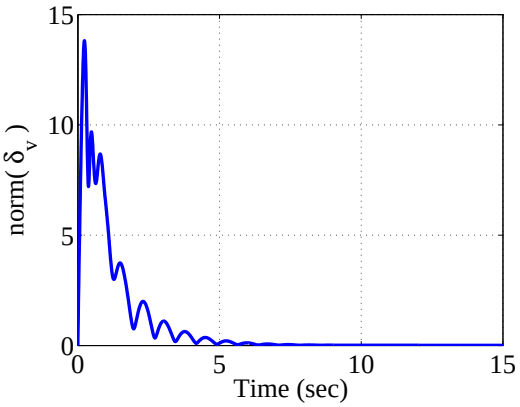

(c) A plot of $\|\delta_v(t)\|$ showing a steady-state velocity error.

Figure 5.4: Without any additional control, tracking a leader leads to a steady-state error in the formation.

in (5.31) will be

$$\begin{aligned}
\dot{\bar{x}} &= \frac{1}{n}\left(\mathbf{1}_n^{\mathrm{T}} \otimes I_2\right)\dot{x} = \frac{1}{n}\left(\mathbf{1}_n^{\mathrm{T}} \otimes I_2\right)v \\
\dot{\bar{v}} &= \frac{1}{n}\left(\mathbf{1}_n^{\mathrm{T}} \otimes I_2\right)\dot{v} \\
&= \frac{1}{n}\left(\mathbf{1}_n^{\mathrm{T}} \otimes I_2\right)\left[-R(x)^T\delta_e - (L \otimes I)\,\delta_v + Bv_{ref}\right] \\
&= \frac{1}{n}\left(\mathbf{1}_n^{\mathrm{T}} \otimes I_2\right)Bv_{ref}
\end{aligned} \tag{5.32}$$

In the case that only one agent is being controlled (i.e., $(\mathbf{1}_n^{\mathrm{T}} \otimes I_2)B = I_2$), the centroid dynamics reduces to

$$\begin{aligned}
\dot{\bar{x}} &= \bar{v} \\
\dot{\bar{v}} &= \frac{1}{n}v_{ref}
\end{aligned} \tag{5.33}$$

© Technion - Israel Institute of Technology, Elyachar Central Library

Moreover, (5.32) reveals that the acceleration of the centroid is proportional to the reference velocity. In particular, when $v_{ref} = const$, the centroid will accelerate at a constant velocity equals to $\frac{1}{n}\left(\mathbf{1}_n^{\mathrm{T}} \otimes I_2\right) B v_{ref}$, concluding the proof. □

As evidence, the leader in the formation described in Figure 5.4(a) is injected with external constant velocity $v_{ref} = \begin{bmatrix} 2 \\ -2 \end{bmatrix}$. The acceleration of the centroid is $\dot{\bar{v}} = \begin{bmatrix} 1/3 \\ -1/3 \end{bmatrix}$ which is consistent with the proof.

5.2.1 Leader's Velocity Feedback Control

As can be seen, the formation is not driven by the velocity reference in the way we want. In the second order system, the purpose of v_{ref} is to determine the velocity of the formation as a whole, meaning that each agent should have a steady state velocity equal to v_{ref}.

For that purpose we want to find a decentralized control to manipulate the velocity of the agents according to v_{ref}. Without loss of generality, we assume that agent number 1 is the leader and is driven by an inner control loop such that its velocity will attain the reference velocity. The remaining agents are not aware of the external reference velocity and are manipulated only by their own preceding dynamics as in (5.34)

$$\begin{aligned} u_1(t) &= -\sum_{j\sim 1}\left(\|e_k\|^2 - {d_k}^2\right) e_k - \sum_{j\sim 1}\left(v_j - v_1\right) + v_{ref} - v_1 \\ u_i(t) &= -\sum_{j\sim i}\left(\|e_k\|^2 - {d_k}^2\right) e_k - \sum_{j\sim i}\left(v_j - v_i\right) \quad \forall i \neq 1. \end{aligned} \tag{5.34}$$

The closed loop dynamics can be written in state space form as:

$$\begin{aligned} \dot{x} &= v \\ \dot{v} &= -R(x)^T\left(R(x)x - d\right) - \left(L \otimes I\right) v + B v_{ref} - BB^T v, \end{aligned} \tag{5.35}$$

where $BB^T \in \mathbb{R}^{2n\times 2n}$ is a block diagonal matrix and is used to indicate that the feedback comes from the agent that has received the external velocity reference, $v_{ref} \in \mathbb{R}^2$ (i.e., if agent i is the leader, then the ith diagonal block of BB^T is I_2, and the remaining blocks are zero). Such control scheme is also depicted in Figure 5.5.

© Technion - Israel Institute of Technology, Elyachar Central Library

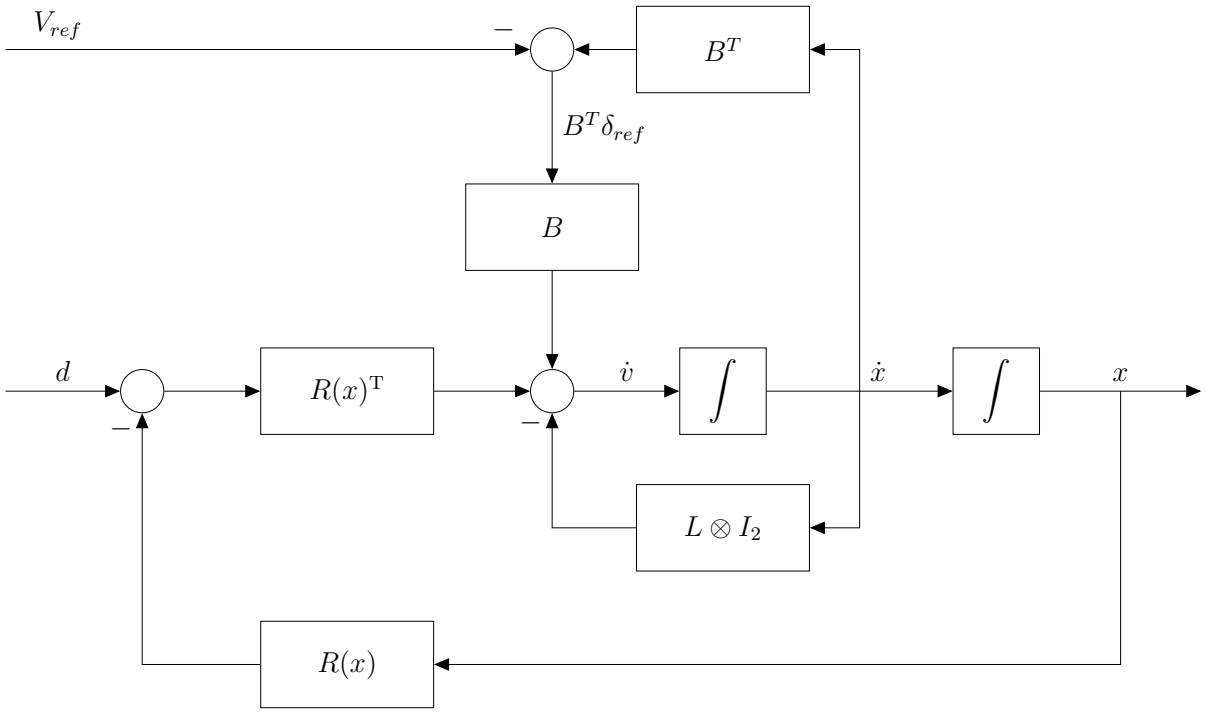

Figure 5.5: Velocity feedback mechanism to ensure velocity tracking of v_{ref}.

5.2.2 Stability Analysis

In this section the stability of the second order system described in (5.35) with the feedback controller is analyzed and discussed. It is shown that the system is locally asymptotically stable.

Intuitively, in order to do that, we define the following error

$$\delta_{ref} = v - (\mathbf{1}_n \otimes I_2)\, v_{ref}. \tag{5.36}$$

The error δ_{ref} belongs to $\mathbb{R}^{2n}$ and states the difference between the velocity of each agent to the reference velocity v_{ref}. It is also presented in Figure 5.6, together with δ_e as an observable output of the second order system with a reference velocity command in (5.31).

© Technion - Israel Institute of Technology, Elyachar Central Library

© Technion - Israel Institute of Technology, Elyachar Central Library

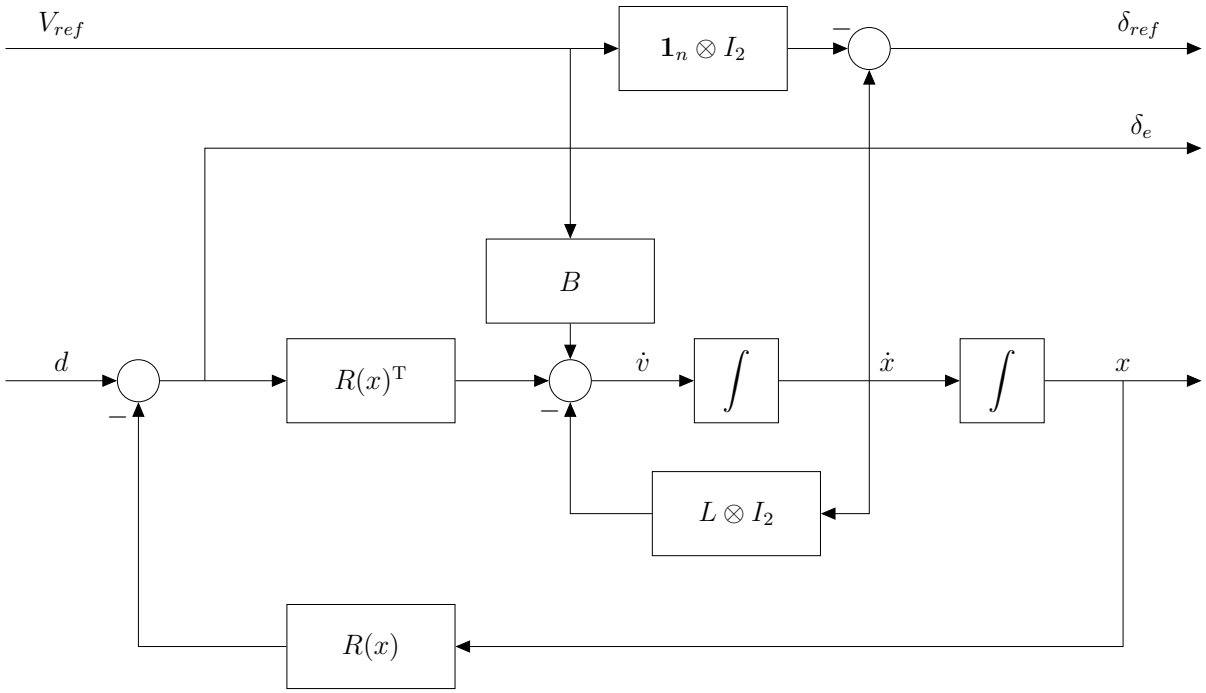

Figure 5.6: The second order system with a velocity reference command.

With the help of matrix $B \in \mathbb{R}^{2n\times 2}$, (5.36) can be manipulated to present the velocity error for the leader:

$$B^T \delta_{ref} = B^T v - v_{ref}. \tag{5.37}$$

where $B^T (\mathbf{1}_n \otimes I_2) = I_2$ is the unit coefficient of v_{ref} and $B^T \delta_{ref}$ is noted in Figure 5.5.

For a constant reference velocity, the dynamics of (5.35) can be written in terms of the defined errors by using (5.13) and (5.37):

$$\begin{aligned} \dot{x} &= v \\ \dot{v} &= -R(x)^T \delta_e - (L \otimes I)\, v - BB^T \delta_{ref}, \end{aligned} \tag{5.38}$$

and it will be useful in our journey to prove stability using Lyapunov's direct method.

Before analyzing the stability of the system, we show that for the dynamics in (5.38), the acceleration of the formation centroid is proportional to the reference error of the leader. In order to examine the connection between the centroid dynamics to the new defined reference error, analysis of the centroid dynamics equation is needed.

Theorem 14. *Consider the closed loop system (5.38) with a reference velocity v_{ref}. Then the centroid of the formation, (3.9), moves at the acceleration $-\frac{1}{n} B^T \delta_{ref}$.*

© Technion - Israel Institute of Technology, Elyachar Central Library

Proof. Implementing the formation dynamics (5.38) into (3.9):

$$\begin{aligned} \bar{v} &= \frac{1}{n}\left(\mathbf{1}_n^{\mathrm{T}} \otimes I_2\right)\dot{x} = \frac{1}{n}\left(\mathbf{1}_n^{\mathrm{T}} \otimes I_2\right)v \\ \bar{a} &= \frac{1}{n}\left(\mathbf{1}_n^{\mathrm{T}} \otimes I_2\right)\dot{v} \\ &= \frac{1}{n}\left(\mathbf{1}_n^{\mathrm{T}} \otimes I_2\right)\left[-R(x)^T\delta_e - (L \otimes I_2)\,v - BB^T\delta_{ref}\right]. \end{aligned} \tag{5.39}$$

First, the velocity of the centroid is independent of the v_{ref} (at least implicitly), and equal to the average of the agents' velocities. Secondly, in the proof of Theorem 10 it was shown that $\mathbf{1}_n$ belongs to the left null space of $R(x)^T$ and L, hence,

$$\bar{a} = -\frac{1}{n}\left(\mathbf{1}_n^{\mathrm{T}} \otimes I_2\right)BB^T\delta_{ref} = -\frac{1}{n}B^T\delta_{ref}. \tag{5.40}$$

It can be seen that the acceleration of the centroid is depended on the leader's velocity and on the reference velocity. When the expression $B^T\delta_{ref}$ converges to zero, the velocity of the centroid will be constant (zero acceleration). Note also that $B^T\delta_{ref} = 0$ means that the leader is moving at the same speed as the velocity reference. □

Remark 2. *By using the velocity control law in (5.17) we have shown velocity consensus that caused $\delta_v = 0$, i.e. $v_1 = \bar{v}$. Assuming the 5.34 is a stabilizing controller, by combining leader's inner controller with (5.17) we can conclude that the centroid's velocity will be equal to the reference velocity ($\bar{v} = v_{ref}$).*

The stability of the system is shown by using Lyapunov's Direct Method and by using the dynamics of the formation error descibed in (4.2) and the reference error described in (5.36).

The formation error dynamics defined in (4.2) has not changed, i.e., $\dot{\delta}_e = 2R(x)v$. Furthermore, by using (5.36) along with the fact that $\mathbf{1}_n$ belongs to the right null space of $R(x)^T$, the derivative of δ_e can be written as:

$$\dot{\delta}_e = 2R(x)\delta_{ref}. \tag{5.41}$$

Next, we derivate the reference-centroid error, δ_{ref}, defined in (5.36) with a constant reference velocity:

$$\dot{\delta}_{ref} = \dot{v}. \tag{5.42}$$

Theorem 15. *Under Assumption 1, formation error dynamics (5.41) and the reference error dynamics (5.42) are locally asymptotically stable.*

Proof. To show the stability of system (5.38) we use the Lyapunov direct method with the following Lyapunov function:

$$W = \frac{1}{4}\delta_e^T\delta_e + \frac{1}{2}\delta_{ref}^T\delta_{ref}. \tag{5.43}$$

where W is continuously differentiable in δ_e and in δ_{ref}. The derivative of (5.43) yields

$$\dot{W} = \underbrace{\frac{1}{2}\delta_e^T \dot{\delta}_e}_{A} + \underbrace{\delta_{ref}^T \dot{\delta}_{ref}}_{B}. \tag{5.44}$$

According to (5.13) and (5.41), expression A is

$$\frac{1}{2}\delta_e^T \dot{\delta}_e = \frac{1}{2}\delta_e^T 2R(x)v = \delta_e^T R(x)\delta_{ref}, \tag{5.45}$$

and from (5.42) expression B is

$$\begin{aligned} \delta_{ref}^T \dot{\delta}_{ref} &= \delta_{ref}^T \dot{v} \\ &= \delta_{ref}^T \left[-R(x)^T \delta_e - (L \otimes I)\, v - BB^T \delta_{ref}\right] \\ &= -\delta_{ref}^T R(x)^T \delta_e - \delta_{ref}^T (L \otimes I)\, v - \delta_{ref}^T BB^T \delta_{ref}. \end{aligned} \tag{5.46}$$

According to the definition of δ_{ref}, i.e., (5.36), and the fact that $\mathbf{1}_n$ belongs to the left null space of L:

$$\delta_{ref}^T (L \otimes I)\, v = \left[v^T - v_{ref}^T \left(\mathbf{1}_n^T \otimes I_2\right)\right](L \otimes I)\, v = v^T (L \otimes I)\, v. \tag{5.47}$$

By using (5.47), (5.46) can now be written as:

$$\delta_{ref}^T \dot{\delta}_{ref} = -\delta_{ref}^T R(x)^T \delta_e - v^T (L \otimes I)\, v - \delta_{ref}^T BB^T \delta_{ref}. \tag{5.48}$$

By introducing (5.45) and (5.48) into (5.44):

$$\dot{W} = \delta_e^T R(x)\delta_{ref} - \delta_{ref}^T R(x)^T \delta_e - v^T (L \otimes I_2)\, v - \delta_{ref}^T BB^T \delta_{ref}, \tag{5.49}$$

we can write down the derivative of the Lyapunov function in its simplified form by using (5.36):

$$\dot{W} = -v^T (L \otimes I_2)\, v - \left(B^T v - v_{ref}\right)^T \left(B^T v - v_{ref}\right). \tag{5.50}$$

Hence, the time derivative of W is negative semidefinite ($\dot{W} \leq 0$). It is not strictly negative definite because $\dot{W} = 0$ for any $v \in S_2$, where $S_2 = \left\{v \middle| (L \otimes I_2)\, v = 0, B^T v - v_{ref} = 0\right\}$. That means the origin is a stable equilibrium, but not necessarily asymptotically stable. The set S_2 also implies a velocity consensus, i.e., $v_1 = v_2 = ... = v_n$. Moreover, $B^T v - v_{ref}$ can only be zero in one point which implies $v_1 = v_{ref}$. The equation $B^T v - v_{ref} = 0$ together with $(L \otimes I_2)\, v = 0$ means that every agent will have the same velocity equals to the reference velocity. The set S_2 can be written in terms of δ_{ref} by using (5.47):

$$S_2 = \left\{\delta_{ref} \middle| (L \otimes I_2)\, \delta_{ref} = 0, B^T \delta_{ref} = 0\right\}.$$

© Technion - Israel Institute of Technology, Elyachar Central Library

© Technion - Israel Institute of Technology, Elyachar Central Library

LaSalle's invariance principle implies that the errors converge to a set of configurations S_2. Furthermore for a constant reference velocity, in S_2, $v_1 = v_{ref}$, and $v_i = v_j \ \forall i$. Thus, we can conclude that $\delta_{ref} = 0$. Accordingly, from (5.38) and (5.42) the velocity error dynamics is:

$$\dot{\delta}_{ref} = -R(x)^T \delta_e = 0. \tag{5.51}$$

For a MIR graphs R is a full row rank, δ_e must be zero in order for the last equation to hold. The conclusion is that the trajectories will converge to the largest invariant set

$$\left\{(\delta_e, \delta_{ref}) \,|\, \delta_e = 0\,,\ \delta_{ref} = 0\,, B^T \delta_{ref} = 0 \ \forall i\right\}$$

and at least asymptotically the control goal is achieved. □

Finally, the next theorem deals with the centroid's dynamics at steady state, once the stability has been shown.

Theorem 16. *Consider the closed loop system (5.38) with a constant reference velocity v_{ref}. Then the centroid of the formation, (3.9), moves with a constant velocity equals to v_{ref}.*

Proof. In Theorm 14 it was shown that the acceleration is equal to $-\frac{1}{n} B^T \delta_{ref}$. For a constant reference velocity, Theorem 15 describes that by using Lyapunov's Direct Method, the origin of the system is stable and that $\delta_{ref} = 0$ at steady state. By using both Theorems:

$$\bar{a} = 0,$$

and the centroid moves at a constant velocity. Since Theorem 15 also tells that $v_i = v_{ref} \ \forall i$, the centroid moves at a constant velocity equals to v_{ref}.

□

5.2.3 Simulations

In order to demonstrate Theorem 15 consider for example a 6 agents system, in which each agent is implemented with a distributed control law as in (5.37). As can be seen in Figure 5.7(a), for an arbitrary initial positions (depicted in grey), the formation reaches the desired hexagon shape (depicted with bold lines). The norm of the formation error is plotted in Figure 5.7(b) showing that there is no steady state formation error. Also, the norm of the reference error is plotted in Figure 5.7(c) showing zero steady state error, which implies that the velocities of the agents are equal to v_{ref}, supporting Theorem 16.

© Technion - Israel Institute of Technology, Elyachar Central Library

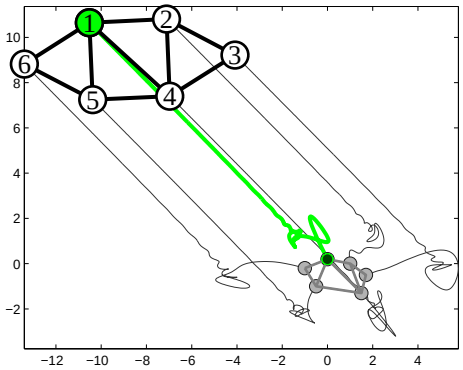

(a) An MIR formation tracking a leader.

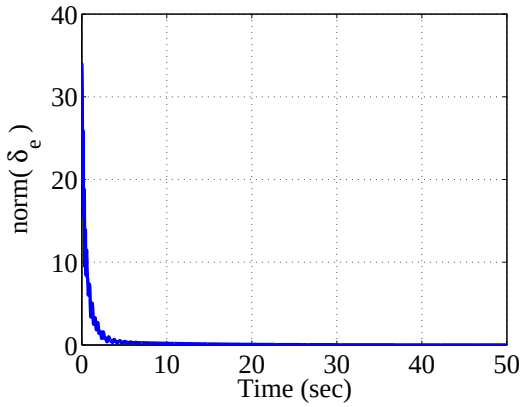

(b) A plot of $\|\delta_e(t)\|$ showing a steady-state distance error.

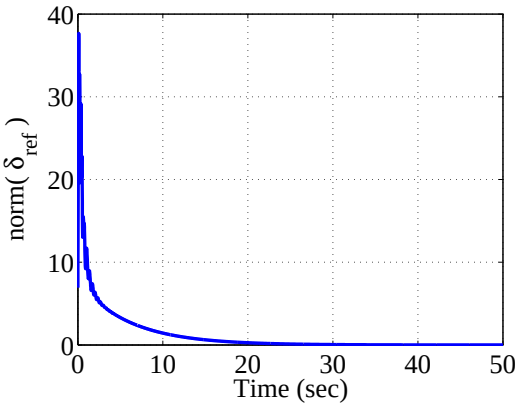

(c) A plot of $\|\delta_{ref}(t)\|$ showing a steady-state velocity error.

Figure 5.7: Tracking a leader with a zero steady-state errors.

© Technion - Israel Institute of Technology, Elyachar Central Library

© Technion - Israel Institute of Technology, Elyachar Central Library

Chapter 6

Conclusions

This work considers a multi-agent formation control problem where a designated leader is subjected to an additional velocity reference command. The entire formation should follow the leader while maintaining the inter-agent distance constraints. The formation error is defined from the zero-input dynamics of agents modeled as single integrators.

By augmenting a standard gradient formation controller with a proportional-integral control on the formation error, we are able to prove the stability of the formation error dynamics with velocity input while ensuring zero steady-state formation error. In order to solve the formation tracking problem of a multi-agent system, we augmented a distance-based rigidity control law with a PI controller on the formation error. We started with agents modeled as single integrators and demonstrated that the stability of the distance error dynamics can be proven using Lyapunov's indirect method. The centroid of the first order system moves at a speed proportional to the reference velocity.

By finding an expression for the steady state formation error of the linearized dynamics, we show that the error properties are related to the graph topology. By simulations, we showed that the formation error vector can be manipulated, and eventually converges to zero, and that the formation tracks the leader with a reference velocity.

To agents with double integrator dynamics we added a consensus-based control loop on the velocities to achieve the formation maintenance problem. The formation error is augmented with a velocity error, that defines the differences between the velocity of each agent to that of the reference. Lyapunov's second method is used to prove that the system is asymptotically stable. For a system with an external reference velocity a decentralized control is proposed to manipulate the agents' velocities and a velocity feedback mechanism is implemented on the leader to assure the formation tracks the reference signal. Numerical simulations were shown to illustrate the theoretical results.

6.1 Future Work

While this thesis has demonstrated how to control a formation of agents when one of them is subjected to an external reference velocity, many opportunities for extending the scope of this thesis remain. This section presents some of these directions.

Finding the relation of $M(x^*)^{-1}$ to the graph

In Corollary 2 at Chapter 4 the steady state error was presented for a constant velocity reference, $v_{ref} = v$. The norm of error is bounded by a value that was related to the graph properties:

$$\|\delta_{ss}\| \leq || \frac{\sqrt{d_{max} \cdot \lambda_{max}(L(\mathcal{G}))}}{\lambda_{min}(M(x^*))} \|v\| . \tag{6.1}$$

We have been working on finding the missing graph interpretation of $M(x^*)^{-1}$, where $M(x^*)$ is invertible since it is symmetric positive definite matrix.

One direction of research is to use the condition number of a matrix and analyze this. Denote $\kappa(M(x^*))$ as the condition number of a matrix $M(x^*)$, i.e. $\kappa(M(x^*)) = \frac{\lambda_{max}(M(x^*))}{\lambda_{min}(M(x^*))}$, where $\lambda_{min}(M(x^*))$ is the smallest eigenvalue of $M(x^*)$ that is not zero. By definition,

$$\kappa(M(x^*)) = \|M(x^*)\| \cdot \left\|M(x^*)^{-1}\right\| ,$$

and hence

$$\left\|M(x^*)^{-1}\right\| = \frac{\lambda_{max}(M(x^*))}{\|M(x^*)\| \, \lambda_{min}(M(x^*))} = \frac{1}{\lambda_{min}(M(x^*))}. \tag{6.2}$$

In this direction, further investigation is needed in order to connect $\lambda_{min}(M(x^*))$ to the graph properties.

Multiple leaders

Some work has been done regarding formation maintenance with multiple leaders [43, 53], but there is a place for further improvements regarding the issue of formation tracking. In a case that we have more than one leader we can no longer expect that the formation will track the directions of the velocity references, but we hope the formation will reach its desired shape.

Figure 6.1(a) illustrates how two opposite agents (marked with green) are injected with a reference velocity of the same magnitude, but with opposite directions (right and left). The PI control law is implemented at the agents. The initial conditions are chosen such that the formation is in its desired shape, meaning that the distances constraint are satisfied. The grey dotted lines are the trajectories of the agents, and those appear in the figure as a solid lines

© Technion - Israel Institute of Technology, Elyachar Central Library

due to repeated tracks. The dotted red lines represent the distances between the agents at time $t = 8\ [sec]$ in order to emphasize the transition shape. In this scenario, the average steady state velocity is zero, and results in a non-moving centroid. Further analysis of the centroid's dynamics is needed in order to foresee its behavior in different cases. Figure 6.1(b) shows that the formation will converge to the desired formation shape, despite the transient occurrence caused by the reference velocities. This fact should be proven for this case, and also for the general case of multiple leaders.

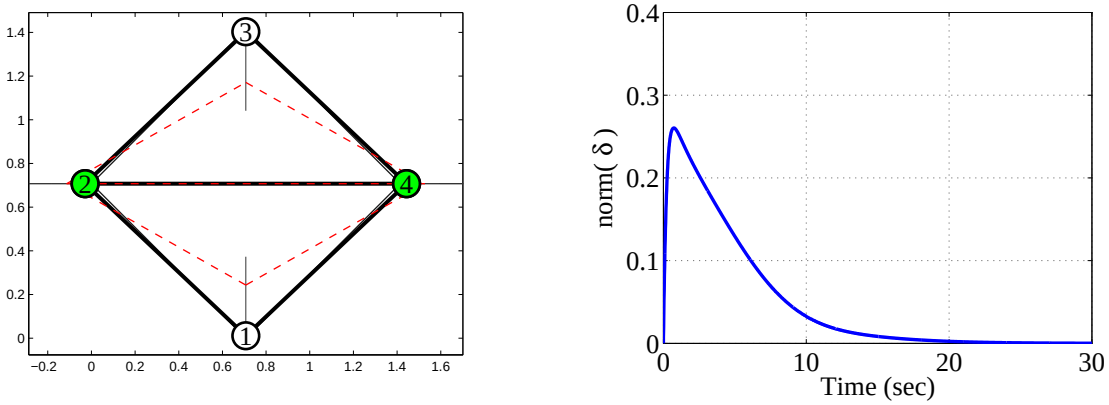

(a) The formation with both agents 2 and 4 as leaders.

(b) The formation error norm, $\|\delta\|$.

Figure 6.1: The norm of the formation tracking error with an upper bound

Different control aproach

It would be interesting to extend and examine some different types of stabilizing controllers in order to search for optimal control in the sense of rate of convergence, disturbance rejections and performance.

For example, consider the classic second-order consensus protocol [35] of the form:

$$\begin{bmatrix} \dot{x}_i(t) \\ \dot{v}_i(t) \end{bmatrix} = \begin{bmatrix} 0 & 1 \\ -L(G) & -L(G) \end{bmatrix} \begin{bmatrix} x_i(t) \\ v_i(t) \end{bmatrix} \tag{6.3}$$

This kind of system employs a Laplacian Based control to reach velocity consensus as well as position consensus. We now apply the same technique to check if rigidity consensus may be achieved by using similar techniques. Consider the system:

$$\begin{bmatrix} \dot{x}_i(t) \\ \dot{v}_i(t) \end{bmatrix} = \begin{bmatrix} 0 & 1 \\ -R(x)^T R(x) & -R(x)^T R(x) \end{bmatrix} \begin{bmatrix} x_i(t) \\ v_i(t) \end{bmatrix} + \begin{bmatrix} 0 \\ R(x)^T \end{bmatrix} d \tag{6.4}$$

© Technion - Israel Institute of Technology, Elyachar Central Library

which can be written as:

$$\begin{aligned} \dot{x}_i(t) &= v_i(t) \\ \dot{v}_i(t) &= -R(x)^T \left[R(x)x(t) - d\right] - R(x)^T R(x) v(t) \end{aligned}$$

From Figure 6.1 we can see that the system is stable and that the desired distances are maintained, but mathematical proof is needed.

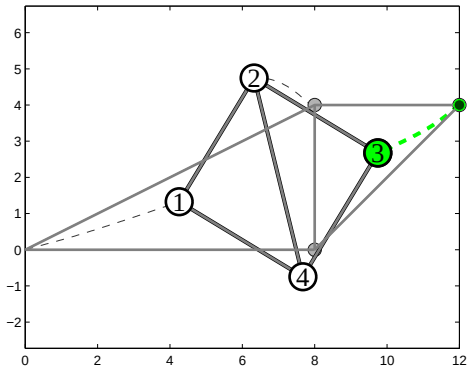

Figure 6.2: The formation with 4 agents - no external velocity.

In the first order system we saw that we can use linearization in order to proof the stability of the error dynamics. In this direction, applying classical linear control methods such as Bode, Nyquist, etc., on the formation control may reveal additional interesting properties.

Extending the control analysis of this work to include dynamic uncertainty in both the agent's system representation and the connection graph may lead to a better understanding and intuition of these systems.

© Technion - Israel Institute of Technology, Elyachar Central Library

© Technion - Israel Institute of Technology, Elyachar Central Library

Bibliography

[1] Abdo Y Alfakih. On the dual rigidity matrix. *Linear Algebra and its Applications*, 428(4):962–972, 2008.

[2] Brian Anderson, Bariş Fidan, Changbin Yu, and Dirk Walle. UAV formation control: Theory and application. In *Recent Advances in Learning and Control*, pages 15–33. Springer, 2008.

[3] Brian Anderson, Changbin Yu, Baris Fidan, and J Hendrickx. Rigid graph control architectures for autonomous formations. *IEEE Control Systems Magzine*, 28(6):48–63, 2008.

[4] Martin Andreasson, Dimos V Dimarogonas, Henrik Sandberg, and Karl H Johansson. Distributed control of networked dynamical systems: Static feedback, integral action and consensus. *IEEE Transactions on Automatic Control*, 59(7):1750–1764, 2014.

[5] Leonard Asimow and Ben Roth. The rigidity of graphs. *Transactions of the American Mathematical Society*, 245:279–289, November 1978.

[6] Leonard Asimow and Ben Roth. The rigidity of graphs, II. *Journal of Mathematical Analysis and Applications*, 68(1):171–190, March 1979.

[7] Nuno Barreto, Luís Macedo, and Licínio Roque. Multiagent system architecture in orphibs ii. In *ALIFE 14: The Fourteenth Conference on the Synthesis and Simulation of Living Systems*, volume 14, pages 3–5.

[8] Mohamed Ali Belabbas. On global feedback stabilization of decentralized formation control. In *50th IEEE Conference on Decision and Control and European Control Conference (CDC-ECC)*, pages 5750–5755, 2011.

[9] Mike Brookes. *The Matrix Reference Manual*. Imperial College, London, UK, 2005.

[10] Birgit Burmeister, Afsaneh Haddadi, and Guido Matylis. Application of multi-agent systems in traffic and transportation. In *IEEE Proceedings on Software Engineering*, volume 144, pages 51–60. IET, 1997.

© Technion - Israel Institute of Technology, Elyachar Central Library

[11] Yongcan Cao, Daniel Stuart, Wei Ren, and Ziyang Meng. Distributed containment control for multiple autonomous vehicles with double-integrator dynamics: algorithms and experiments. *IEEE Transactions on Control Systems Technology*, 19(4):929–938, 2011.

[12] Paresh Deshpande, Prathyush P Menon, Christopher Edwards, and Ian Postlethwaite. Formation control of multi-agent systems with double integrator dynamics using delayed static output feedback. In *50th IEEE Conference on Decision and Control and European Control Conference (CDC-ECC)*, pages 3446–3451. IEEE, 2011.

[13] Dimos V Dimarogonas and Karl H Johansson. Stability analysis for multi-agent systems using the incidence matrix: Quantized communication and formation control. *Automatica*, 46(4):695–700, 2010.

[14] Dimos V Dimarogonas and Karl Henrik Johansson. On the stability of distance-based formation control. In *47th IEEE Conference on Decision and Control (CDC)*, pages 1200–1205. IEEE, 2008.

[15] Florian Dorfler and Bruce Francis. Formation control of autonomous robots based on cooperative behavior. In *European Control Conference (ECC)*, pages 2432–2437. IEEE, 2009.

[16] Tolga Eren. Formation shape control based on bearing rigidity. *International Journal of Control*, 85(9):1361–1379, 2012.

[17] Tolga Eren, Peter N Belhumeur, Brian DO Anderson, and A Stephen Morse. A framework for maintaining formations based on rigidity. In *the 15th IFAC World Congress*, pages 2752–2757, Barcelona, Spain, 2002.

[18] Miroslav Fiedler. Algebraic connectivity of graphs. *Czechoslovak mathematical journal*, 23(2):298–305, 1973.

[19] C. Godsil and G. Royle. *Algebraic Graph Theory*. Springer, New York, 2001.

[20] Hassan K Khalil. *Nonlinear Systems (Third edition)*. Prentice Hall, 2002.

[21] Laura Krick. *Application of Graph Rigidity in Formation Control of Multi-Robot Networks*. PhD thesis, University of Toronto, 2007.

[22] Laura Krick, Mireille E Broucke, and Bruce A Francis. Stabilisation of infinitesimally rigid formations of multi-robot networks. *International Journal of Control*, 82(3):423–439, 2009.

© Technion - Israel Institute of Technology, Elyachar Central Library

[23] D. A. Burbano Lombana and M. di Bernardo. Distributed pid control for consensus of homogeneous and heterogeneous networks. *IEEE Transactions on Control of Network Systems*, 2(2):154–163, June 2015.

[24] Pattie Maes. Artificial life meets entertainment: lifelike autonomous agents. *Communications of the ACM*, 38(11):108–114, 1995.

[25] Mehran Mesbahi and Magnus Egerstedt. *Graph theoretic methods in multiagent networks*. Princeton University Press, 2010.

[26] Richard M Murray, Zexiang Li, S Shankar Sastry, and S Shankara Sastry. *A mathematical introduction to robotic manipulation*. CRC press, 1994.

[27] Rudy R Negenborn, Bart De Schutter, and J Hellendoorn. Multi-agent model predictive control for transportation networks: Serial versus parallel schemes. *Engineering Applications of Artificial Intelligence*, 21(3):353–366, 2008.

[28] Sergio Ocio and Jose Antonio Lopez Brugos. Multi-agent systems and sandbox games. In *University of Oviedo*. Citeseer, 2008.

[29] Katsuhiko Ogata. *Modern Control Engineering Fourth Edition*. Prentice Hall PTR, 2002.

[30] Reza Olfati-Saber. Flocking for multi-agent dynamic systems: Algorithms and theory. *IEEE Transactions on Automatic Control*, 51(3):401–420, 2006.

[31] Reza Olfati-Saber and Richard M Murray. Graph rigidity and distributed formation stabilization of multi-vehicle systems. In *the 41st IEEE Conference on Decision and Control*, volume 3, pages 2965–2971, 2002.

[32] Michal Pěchouček and Vladimír Mařík. Industrial deployment of multi-agent technologies: review and selected case studies. *Autonomous Agents and Multi-Agent Systems*, 17(3):397–431, 2008.

[33] Jeremy Pitt, Brendan Neville, Sam Macbeth, and Hugo Carr. Animation of open multi-agent systems. In *SPRINGSIM*, 2011.

[34] Wei Ren. Consensus strategies for cooperative control of vehicle formations. *IET Control Theory & Applications*, 1(2):505–512, 2007.

[35] Wei Ren and Ella Atkins. Second-order consensus protocols in multiple vehicle systems with local interactions. In *AIAA Guidance, Navigation, and Control Conference*, pages 15–18, 2005.

© Technion - Israel Institute of Technology, Elyachar Central Library

[36] Wei Ren and Randal W Beard. *Distributed consensus in multi-vehicle cooperative control*. Springer, 2008.

[37] Oshri Rozenheck, Shiyu Zhao, and Daniel Zelazo. Distance-constrained formation tracking control. In *Israel 55th Annual Conference on Aerospace Sciences*, 2015.

[38] Oshri Rozenheck, Shiyu Zhao, and Daniel Zelazo. A proportional-integral controller for distance-based formation tracking. In *European Control Conference (ECC)*, pages 1693–1698. IEEE, 2015.

[39] David A Sanchez. *Ordinary differential equations and stability theory: an introduction*. Courier Corporation, 1968.

[40] Shankar Sastry. *Nonlinear systems: analysis, stability, and control*, volume 10. Springer Science & Business Media, 2013.

[41] Demetri P Spanos, Reza Olfati-Saber, and Richard M Murray. Dynamic consensus on mobile networks. In *IFAC world congress*, pages 1–6. Citeseer, 2005.

[42] Housheng Su, Xiaofan Wang, and Zongli Lin. Flocking in multi-agent systems with a virtual leader. *IEEE Transactions on Automatic Control*, 54(2):293–307, 2009.

[43] Housheng Su, Xiaofan Wang, and Wen Yang. Flocking in multi-agent systems with multiple virtual leaders. *Asian Journal of control*, 10(2):238–245, 2008.

[44] Herbert G Tanner, Ali Jadbabaie, and George J Pappas. Stable flocking of mobile agents part i: Dynamic topology. In *the 42nd IEEE Conference on Decision and Control*, volume 2, pages 2016–2021, 2003.

[45] Herbert G Tanner, Ali Jadbabaie, and George J Pappas. Flocking in fixed and switching networks. *IEEE Transactions on Automatic Control*, 52(5):863–868, 2007.

[46] Tiong-Seng Tay and Walter Whiteley. Generating isostatic frameworks. *Structural topology*, 11:21–69, 1985.

[47] Parunak H Van Dyke, Sven Brueckner, and John Sauter. Digital pheromone mechanisms for coordination of unmanned vehicles. In *Proceedings of the first international joint conference on Autonomous agents and multiagent systems: part 1*, pages 449–450. ACM, 2002.

[48] Wenwu Yu, Guanrong Chen, and Ming Cao. Some necessary and sufficient conditions for second-order consensus in multi-agent dynamical systems. *Automatica*, 46(6):1089–1095, 2010.

[49] Wenwu Yu, Wei Xing Zheng, Guanrong Chen, Wei Ren, and Jinde Cao. Second-order consensus in multi-agent dynamical systems with sampled position data. *Automatica*, 47(7):1496–1503, 2011.

[50] Daniel Zelazo, Antonio Franchi, Frank Allgöwer, Heinrich H Bülthoff, and Paolo Robuffo Giordano. Rigidity maintenance control for multi-robot systems. In *Robotics: Science and Systems*, 2012.

[51] Daniel Zelazo, Amirreza Rahmani, and Mehran Mesbahi. Agreement via the edge laplacian. In *46th IEEE Conference on Decision and Control*, pages 2309–2314, 2007.

[52] Shiyu Zhao and Daniel Zelazo. Bearing-based formation maneuvering. In *IEEE International Symposium on Intelligent Control (ISIC)*, pages 658–663. IEEE, 2015.

[53] Shiyu Zhao and Daniel Zelazo. Translational and scaling formation maneuver control via a bearing-based approach. *IEEE Transactions on the Control of Network Systems*, PP(99):1–10, 2015.

© Technion - Israel Institute of Technology, Elyachar Central Library

© Technion - Israel Institute of Technology, Elyachar Central Library

תקציר

העבודה עוסקת בשמירת מבנה של מערכות מרובות סוכנים, כאשר הסוכן המנהיג נתון תחת השפעתה של פקודת מהירות חיצונית. על שאר הסוכנים במבנה לעקוב אחר המנהיג ובאותה העת לשמור על אילוצי המרחקים בין הסוכנים. מערכת מרובת סוכנים מורכבת ממספר סוכנים היכולים לתקשר ביניהם בתוך סביבה מסוימת. השימוש במערכות מרובות סוכנים נפוץ בעיקר בבעיות אותן קשה ואפילו בלתי אפשרי לפתור באמצעות סוכן אחד. דוגמאות נפוצות למערכות אלו ניתן למצוא במשחקי מחשב, מערכות הגנה ותקיפה, תחבורה ועוד. הכלי המתמטי המרכזי לטיפול במערכות מרובות סוכנים הוא תורת הגרפים, אשר יוסבר בהרחבה בתחילת העבודה.

עבודה זו תציג איך לבקר מערכות מרובות סוכנים מנקודת מבט של שמירת מבנה. בהקשר זה סוכנים יכולים להיות רובוטים, כלי טיס, לוויינים ועוד. בקרת מבנה באמצעות שמירת אילוצי המרחקים בין הסוכנים מסתמכת על מדידות יחסיות בין הסוכנים בלבד, דהיינו מרחק יחסי ומיקום יחסי עבור מערכת מסדר ראשון ובנוסף מהירות יחסית עבור מערכת מסדר שני). תורת הקשיחות מסתמנת ככלי המתאים ביותר לטיפול בבעיות מסוג זה וכוללת גם את היכולת להראות יציבות עבור חוקי בקרה שונים. באופן כללי, מבנה קשיח הוא מבנה בו תנועת הסוכנים שומרת על המרחקים המוגדרים ביניהם ויוצרת תנועת טרנסלציה או רוטציה של המבנה כולו בלבד. כאשר קיימת כניסת מהירות חיצונית למערכת, חוקי הבקרה נדרשים לספק עקיבת מהירות של המבנה אחר הקלט.

כיום, קיימים מספר חוקי בקרה המסתמכים על מדידות יחסיות שיובילו את המערכת לתצורה המבוקשת. שגיאת המבנה, שמשמעה ההבדל בין התצורה הרצויה לתצורה הנוכחית, מוגדרת על ידי סוכנים בעלי דינמיקה מסדר ראשון כאשר אין כניסות חיצוניות למערכת. תרומה ראשונה של עבודה זו היא הוכחת היציבות המקומית על ידי שימוש בדינמיקת שגיאת המבנה והפעלת השיטה הלא ישירה של ליאפונוב.בהינתן כניסת מהירות חיצונית ובהעדר פקודת בקרה נוספת חוק הבקרה הסטנדרטי יוביל לשגיאת מבנה במצב מתמיד שונה מאפס. השיטה הלא ישירה של ליאפונוב מובילה גם למציאת חסם עליון על השגיאה במצב מתמיד של המערכת לאחר ליניאריזציה, וחושפת יחסים בעלי חשיבות רבה בין תכונות השגיאה לטופוגרפית הגרף. על ידי הרחבת בקר המבנה הסטנדרטי לבקר פרופורציונאלי ואינטגראלי על השגיאה עצמה, ניתן להוכיח יציבות עבור דינמיקת שגיאת המבנה עם כניסת מהירות ובו בזמן להבטיח את איפוס השגיאה במצב מתמיד.

המשך העבודה יעסוק בסוכנים בעלי דינמיקה של אינטגרטור כפול הכפופים לאותם אילוצי מרחקים. נדגים כי באמצעות חוק הבקרה הסטנדרטי המערכת אינה יציבה ולכן נחוץ בקר נוסף. לשם כך נוסיף בקר קונצנסוס (הסכמה) על מהירויות הסוכנים המהווה נדבך חשוב על מנת לעמוד בהגדרות המשימה של שמירת מבנה . כעת, לשגיאת המבנה מצטרפת שגיאת המהירות של כל סוכן, המוגדרת כהפרש בין המהירות של כל סוכן לזו של הכניסה החיצונית. השיטה הישירה של ליאפונוב מסתמנת כיעילה ובעזרתה מוכחת יציבות אסימפטוטית של המערכת. עבור מערכת עם כניסת מהירות חיצונית, שילוב של בקרה מבוזרת על מנת לבקר את מהירויות הסוכנים יחד עם בקרה בחוג סגור על מהירות הסוכן המנהיג תבטיח עקיבה של המבנה אחר המהירות החיצונית הדרושה. הוכחת יציבות במקרה זה תינתן על ידי שימוש בשגיאה המורחבת, הכוללת בתוכה את שגיאת המרחקים של המבנה, שגיאת המהירות של הסוכנים והשגיאה בין מהירות המנהיג לבין מהירות הכניסה החיצונית. סימולציות נומריות מלוות את ההוכחות התאורטיות ומדגימות את מהימנותן.

© Technion - Israel Institute of Technology, Elyachar Central Library

© Technion - Israel Institute of Technology, Elyachar Central Library

המחקר נעשה בהנחייתו של פרופסור דניאל זלזו במסגרת התוכנית הבין יחידתית למערכות אוטונומיות ורובוטיקה.

אני מודה לדיאן ולאונרד שרמן על התמיכה הכספית הנדיבה בהשתלמותי.

© Technion - Israel Institute of Technology, Elyachar Central Library

© Technion - Israel Institute of Technology, Elyachar Central Library

© Technion - Israel Institute of Technology, Elyachar Central Library

בקרה ועקיבה של סוכנים במבנה עם אילוצי מרחקים

חיבור על מחקר

לשם מילוי חלקי של הדרישות לקבלת תואר מגיסטר למדעים במערכות אוטונומיות ורובוטיקה

אושרי רוזנהק

הוגש לסנט הטכניון – מכון טכנולוגי לישראל

ניסן תשע״ו, חיפה, אפריל 2016

© Technion - Israel Institute of Technology, Elyachar Central Library

בקרה ועקיבה של סוכנים במבנה עם אילוצי מרחקים

אושרי רוזנהק

© Technion - Israel Institute of Technology, Elyachar Central Library